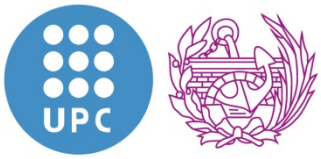

Escola Tècnica Superior d'Enginyers de Camins, Canals i Ports de Barcelona

UNIVERSITAT POLITÈCNICA DE CATALUNYA

PROJECTE O TESINA D'ESPECIALITAT

Títol

Experimental and theoretical study of the capillary effect on the mechanical behaviour of granular media

Autor/a

Carla Moure i Foraster

Tutor/a

Alejandro Josa

Departament

Enginyeria del Terreny, Cartogràfica i Geofísica (ETCG)

Tutors externs

Pierre Lambert (BEAMS (Bio-, Electro- and Mechanical Systems), ULB)

Bertrand François (BATir (Building, Architecture and Town planning), ULB)

Data

“Education and investigation are the only ways to get out of this mess”

Carla Moure

INDEX

DEDICATIONS

The accomplishment of this final thesis was like a trip to an unknown land. Moreover if you write it in a foreign country, in a foreign language, with strangers as tutors, and working on much more theoretical and scientific subjects than anything you have done before. So, yes, it was amazing, but difficult. It was certainly complicated for me to join the subject (firstly because of the language); to be able to understand where I was and where I was supposed to go, knowing which elements concerned me and my thesis and which didn't. In this day and age, the amount of accessible information is so huge, meaning that it is extremely easy "to waste" your time, reading hundreds of articles that you find one after another, why? Because you find one thing that you do not know or understand, so you search for it on Google, and you find an interesting article about that subject, but within that article you find another new concept, so again you search for it on Google, and you find an interesting article about that subject, but within that article you find another new concept… and the cycle continues, as you can see it is an infinite chain, that you have to stop at one time or another, or you will have gained a lot of knowledge but no thesis. I think the most difficult thing is to select the information needed from the amount we currently have at our disposal.

I would like to thank all my traveller companions with all my might on this amazing trip with all its patches, composing all the fundamental pieces of this puzzle called thesis:

- Bertrand François, because if somebody has made this thesis possible is him, without doubt, because it was him who proposed me this work. I would like to thank him for having patience, for understanding and for spending lots of time on me; he has been the mother of my thesis.
- Pierre Lambert, who imposed the discipline and the rigour, becoming the father of my thesis and who gave me a scientific insight. I would also like to thank him for his infinite knowledge (one part of it being expressed in his book [1]; my lantern on this journey), the furniture and the place to stay, at BEAMS, a place where I have met a lot of very kind people.
- Alejandro Josa, for giving me his advice, replying with great interest and kindness to all my doubts and numerous emails. He has been, my most important support, academically this year, why? Because he gave me a boost of self-confidence and motivation, it is comforting to know that the professor, who you admired the most from your home university, has confidence in you.
- Rajan Filomeno Coelho, my Erasmus coordinator and a great person, always willing to listen and for making me calm down and think strategically, when the pressure on me was higher than atmospheric...
- Nicolas Cauche, Jean-Baptiste Valsamis and Marion Sausse Lhernould, for all their help, with the test bed, the MATLAB staff, the printer installation… and, moreover, their friendliness and the good company they were for me at BEAMS.
- Maria Chiara Di Carlo, with her great scientific spirit, gave me an example for what I was supposed to do. I really think she will succeed in all she goes on to do, as her PhD is waiting for her in Canada.
- Michael Tolley and Karim Slaoui, who have helped me to understand the numeric

analysis and its implementation in Matlab, needed for my routine.

- Nicolas Canu and Simon Croegaert, who have made the experiments possible in the Geotechnical laboratory.
- Ivan Puig, who has replied to all my questions, who has given me hundreds of pieces of advice, and thousands of very useful articles, and who deserves several Belgian beers, as he did not know them very well…
- Nikki White, who has given me a lot of her time correcting my English, making me learn "proper stuff" not only on paper, but day after day, improving my oral and converting my English into something more British than the queen!
- Fernando Bache and Francis Daza, for all the service given to me, such as the permanent technical assistance and advising me on choosing a new PC, which has been great.
- Larry Page and Sergey Brin, for making everything so easy by inventing Google.
- Jimmy Wales and Larry Sanger, for having the great and very useful idea of Wikipedia.
- Michael Kellogg, for creating WordReference, whether it being for my French, English or Italian teacher, and making the writing of, not just this paper, but all my work, on this academic year abroad a lot less difficult.
- www.delicieuse-musique.com, www.soundcloud.com, Spotify and YouTube for giving me the energy to work and work and work and work…
- Masy, Rocío, Sophie, Johanne, Célie, Rémi, Maxime, Cédric… who have given me the company and distraction I needed whilst working on this paper.
- Ana, Andrea, Carlos, Claudia, Denise, Emma, Iván, Miriam, Sara and Tamara, for being always there, and for making me feel as though we have never been separated. I hope I will be able to keep them as friends all my live, they are treasures, and it was not easy at all to find them.
- My cousin, Albert Moure, who has been so close to me, although being so far away, and always asking about my progress and who has lots of confidence in me (as my grandfather did when we were both on the same planet), and who will arrive when he wants to, I would put a bet on it!

If I have to be grateful to somebody for being my support, my strength, my psychologists, my advisors, my generous bankers… briefly; the best; it's my parents. ALL I HAVE, MATERIAL OR NOT, IT IS THANKS TO THEM. So, thanks, and the only thing I want is to feel that I have made the most of everything they have given to me, and to know that they are proud of me.

Last but not least, I want to dedicate this work to my little brother Nil, certainly the most important person in my world, and who has been so far from me all year, accepting that fact without arguments… I hope that one day he will write a paper like this, in which I am sure he will do much better than me, given the capacity and attitude he already shows. Now it is your turn, I pass the baton on to you, my sweet. T'ESTIMO NEN

ABSTRACT

Effective stress in unsaturated soils has never been physically or mathematically defined. It is still the topic in large discussions and debates in the soil mechanics community. We therefore tried to obtain a more realistic effective stress distribution within partially saturated conditions deduced from the measurement of capillary forces between spherical particles. We investigated a monodisperse granular material in which the particle interactions are governed by a capillary force law. The cohesion force for a grain-pair with equal diameters is expressed as an explicit function of the liquid bridge (both its volume and its shape). This analytical relation is validated by experiments consisting of measuring the capillary force between two particles joined by a meniscus. A numerical simulation was created by a routine Matlab, to determine the capillary force and the water pressure between two balls in contact with different saturation parameters (given the contact angle), produced by traction micromechanical experiments. Finally, in order to evaluate the influence of capillary force on the macroscopic behaviour, shear strength tests have been carried out using different water contents.

KEY WORDS

Capillarity, liquid bridge, granular media, numerical simulation, experimental approximation, mechanical behaviour, suction, capillary force.

RESUMEN

La tensión efectiva en suelos no saturados nunca ha sido física ni matemáticamente definida y sigue siendo el tema de largas discusiones y debates en el mundo de la mecánica de suelos. En este trabajo tratamos de obtener una distribución más realista de las tensiones efectivas en suelos granulares parcialmente saturados deducida a partir de la medida de las fuerzas capilares entre partículas esféricas. Se ha investigado un material granular monodisperso, cuyas interacciones entre partículas se rigen por una ley de fuerza capilar. La fuerza de cohesión entre un par de granos del mismo diámetro se expresa como una función explícita del puente líquido (tanto de su volumen, como de su forma). Esta relación analítica es validada por experimentos que consisten en la medición de la fuerza capilar entre dos partículas unidas por un menisco. Una simulación numérica fue creada con una rutina de Matlab para determinar la fuerza capilar y la presión de agua entre dos esferas en contacto con diferentes parámetros de saturación (dado el ángulo de contacto) producidas por los experimentos micromecánicos de tracción. Finalmente, con el fin de evaluar la influencia de la fuerza capilar en el comportamiento macroscópico, se han llevado a cabo ensayos de resistencia al cizallamiento utilizando diferentes contenidos de agua.

PALABRAS CLAVE

Capilaridad, puente liquido, medio granular, simulación numérica, aproximación experimental, comportamiento mecánico, succión, fuerza capilar.

RÉSUMÉ

La contrainte effective dans les sols non saturés n'a jamais été physique ou mathématiquement définie. Il reste encore comme sujet dans de grands discussions et débats dans la communauté de mécanique des sols. On a donc essayé d'obtenir une répartition des contraintes effectives plus réaliste avec des conditions partiellement saturées déduite de la mesure des forces capillaires entre des particules sphériques. On a étudié un matériau granulaire monodisperse dans lequel les interactions entre particules sont régies par une loi de force capillaire. La force de cohésion pour un pair de grains avec le même diamètre est exprimé comme une fonction explicite du pont liquide (à la fois de son volume et de sa forme). Cette relation d'analyse est validée par des expériences consistant à mesurer la force capillaire entre deux particules reliées par un ménisque. Une simulation numérique a été créée par une routine Matlab, pour déterminer la force capillaire et la pression d'eau entre deux billes en contact avec des paramètres de saturation différents (étant donné l'angle de contact) produite par des expériences de traction micromécaniques. Enfin, afin d'évaluer l'influence de la cohésion capillaire sur le comportement macroscopique, des tests de résistance au cisaillement ont été réalisées avec de différentes teneurs en eau.

MOTS CLÉS

Capillarité, pont liquide, milieux granulaire, simulation numérique, approximation expérimentale, comportement mécanique, succion, force capillaire.

RESUM

La tensió efectiva en sòls no saturats mai ha estat física ni matemàticament definida i segueix sent el tema de llargues discussions i debats en el món de la mecànica dels sòls. En aquest treball intentem obtenir una distribució més realista de les tensions efectives en sòls granulars parcialment saturats deduïda a partir de la mesura de les forces capil·lars entre partícules esfèriques. S'ha investigat un material granular monodispers; les interaccions entre partícules es regeixen per una llei de força capil·lar. La força de cohesió entre un parell de grans de mateix diàmetre s'expressa com una funció explícita del pont líquid que els uneix (tant del seu volum, com de la seva forma). Aquesta relació analítica és validada per experiments que consisteixen en la mesura de la força capil·lar entre dues partícules unides per un menisc. Una simulació numèrica s'ha creat amb una rutina de Matlab per determinar la força capil·lar i la pressió d'aigua entre dues esferes en contacte amb diferents paràmetres de saturació (donat l'angle de contacte) produïdes pels experiments micromecànics de tracció. Finalment, per tal d'avaluar la influència de la força capil·lar en el comportament macroscòpic, s'han dut a terme assaigs de resistència al cisallament amb diferents continguts d'aigua.

PARAULES CLAU

Capilaritat, pont liquid, medi granular, simulació numèrica, aproximació experimental, comportament mecànic, succió, força capilar.

INTRODUCTION

This paper provides an estimate of effective stress within non saturated soils, with different percentages of water, both theoretically and experimentally. Two approximations were compared, to contrast the validity of the numeric approximation. The soil can be seen as a set of grains and the effects of water on soil behaviour are the consequences on a macroscopic scale of the phenomena that occurs locally, which is to say, the scale of the soil particle (also called a grain). It is due to this, that within the experimental framework, two approaches were tackled: the setting up of a test bed from a microscopic point of view by analysing capillary cohesion across a pair of grains, then from a macroscopic scale, the accomplishment of direct shear tests with lots of grains (about 5,000) with the same characteristics of those of the pair (i.e. steel balls with a radius of 1 mm). The aim of these two experiments was to compare their results and to evaluate the agreements between them, but unluckily, the technology at our disposal was not as precise as it should have been for the macroscopical experiments, meaning that it produced results that did not have congruence and that had a huge dispersion of the same initial conditions, possibly due to the low sensitivity of the force captor (50 g) compared to the normal force applied to the sample (about 300 grams).

Graphically speaking this project can be broken down as shown in the following diagram:

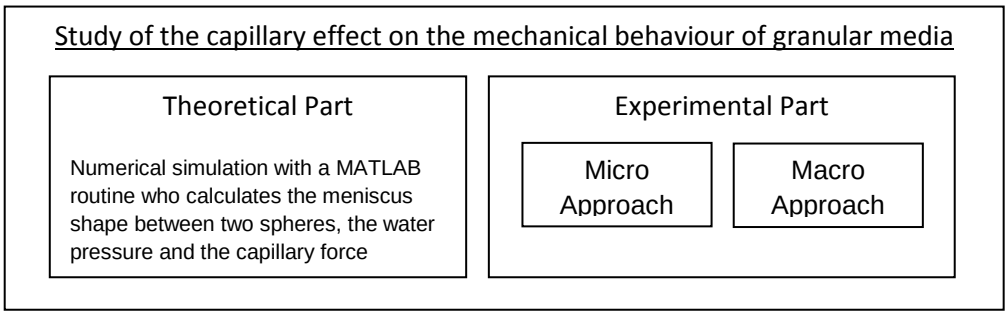

Figure 1: Sketch map of the different parts of the study

In both experimental approaches, the soil was seen as a set of balls; the experiments had to allow measuring traction as well as the shear forces that soil is able to hold, and how they vary in different water contents. The following procedures were used:

- For the microscopic approach, we measured the individual forces between the balls in order to see the interactions between one ball and another. We made traction tests with the displacement precisely controlled, already used by Lambert and Al [1].
- For the macroscopic approach, a container was filled with a few thousand balls and a known amount of liquid. Several experiments were performed using different percentages of water (out of the overall volume). For each experiment, a shear force was transmitted to the layers of balls, in order to displace some compared to others. By doing this, we obtained the average stress values for thousands of balls, as a function of the amount of liquid.

A bed test allowing the measurement of capillary forces in shear strength should have been designed. This work did not suit my field of studies (but that of electro-mechanical civil engineering), and I could not be in charge of that matter, given the finite condition of the time and the already large amount of work given by the initial objectives proposed. This was therefore the project of one student, explained in full further on.

The liquid used within all the parts of this work was distilled, avoiding then, the osmotic suction, and having only the matrix one.

For thirty years, numerical methods opened growing possibilities thanks to the progression of communication technology providing the tools to allow the completion of our knowledge on the granular material. These numerical approaches are numerical models of granular media; they do not take in account the full complexity of real granular media, both in terms of the description of physical phenomena and in terms of geometry and number of grains. However, these methods constitute an effective study tool, allowing a better understanding of granular media physics', presently an increasing issue in science.

The aim of this work is to study the capillary forces between grains of the same size, i.e. monodisperses.

The thesis has 4 main chapters:

1) The state of the art, where is explained complexity of granular media, the effective stress principle and the approximations within unsaturated soils, the roll of the suction and its relation with the moisture, and geometry and surface effects of the grains.
2) The experimental study, compound by:
    a. A part of micro-scale experiments, where is detailed the traction experiment, and the requirements for the shear strength one.
    b. A part of macro-scale experiments, where are explained the characteristics of the shear strength experiments carried out in the Geotechnical Laboratory.
3) The theoretical study, where is called into question the Israelachvili force and the effective stress parameter.
4) The numerical simulation, where are explained the two Matlab routines used, which calculate the meniscus shape between two spheres, the water pressure and the capillary force.

Finally, we found the comparison of the results produced by each method and the possible prospects within this field.

1. STATE OF THE ART

1.1. COMPLEXITY OF GRANULAR MEDIA

This work concerns the study of granular media, which happens to be a certain number of macroscopic objects (called grains) that interact by means of temporary or permanent contact. They are the object of so many studies because they constitute an example of disordered material, which show really curious phenomenon that currently cannot be explained. This ignorance can be explained by the difficulty of reaching local information, at a grain scale, and the imperfect understanding of the relation between local interactions and the macroscopic behaviour of granular media.

Granular media is obviously closely related to soil mechanics, but it is universally distributed in nature and is used in many fields of human activity and is ubiquitous in the many shapes and sizes in our environment. From sand castles to space exploration, passing through the transformation, pharmaceutics and agro-alimentary industries, construction materials, cereal and mineral storage, etc. Granular media takes part in everyday life. Currently, almost 80% of products (or intermediary) for process industries happen to be in grain or powder form, it is due to this, the advances related to the behaviour of these materials have an important potential [2].

Faced with the complexity of the media in question and to be able to study the capillarity cohesion more easily, we considered an ideal granular media, based on the following hypothesis:

1) The grains were taken to be spherical and perfectly smooth (no roughness).

2) The grains were supposed of the same nature, meaning that their properties, both physical and chemical, are self-same. The grains were therefore supposed to be constituted of the same material and be monodisperse.

Unsaturated soils represent an important three-phase system in which internal forces arise from the interaction of solid, liquid and gas phases. If we study the soil deeply, we can see that, contrary to what they have taught at university (Figure 2), there are not only three phases, but that an air-water interface is generated by capillarity effects in the meniscus that is formed between the adjacent soil particles. Therefore, it must be considered that this contractile skin formed between the gas and the liquid phase, is a fourth phase in the study of stress conditions, as depicted in Figure 3. As such, in determining the behaviour and strength of unsaturated soils, it becomes difficult to choose the controlling stress variable that would substitute for the role of effective stress in the saturated case.

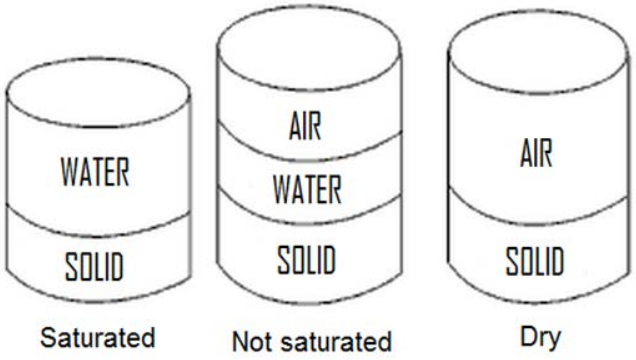

Figure 2: The different soil states seen simply

We know the behaviour of saturated soil very well (that is to say, one that is composed of only two phases, the solid and the liquid, meaning all the voids are filled with water) with the effective stress concept, being part of the classical soil mechanics, and the result of the laboratory experiments produced by Karl von Terzaghi in 1936, which provided essential relations in soil mechanics, allowing predictions on its behaviour. As said by von Terzaghi, the effective stress, id est the intergranular average stress carried by the soil skeleton, may be calculated as the simple subtraction of the pore pressure from the overall stress. For him, the term 'effective' meant that the calculated stress was effective in moving soil, or causing displacements. Mechanical effects, are defined by total and interstitial pressure, their effects are associated with volume changes and shear strength within saturated or dry soils. It is important to distinguish between the terms stress and pressure. By definition, the pressure on a point is the same in all directions, whereas the stress can be different in each given direction. Within soil mechanics, the compressive stresses are considered to be positive and those of traction as negative, which has to be reminded to those who are more used to the solid mechanics criterion, which uses exactly the opposite theory.

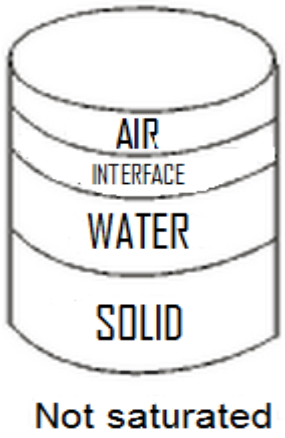

Figure 3: The real phases

The problem is that soil is not always found as saturated and, it is at that point where we do not know how to accurately define its mechanical behaviour. It is not by sheer chance that the study of soil mechanics has been focused on saturated soils, rather that we can say there are "good" reasons that justify this fact: firstly because saturated soils are abundant in developed countries with temperate climates; secondly because the effective stress principle assumes a proper reference framework and, lastly, because, in many cases, the saturated condition – which tends to be the worst – is a predictable situation across the lifespan of preservation works, such as on foundations, embankments, canals…

In the world of the mechanics of unsaturated soils, there are two different constitutive frameworks to characterise the mechanical behaviour of granular media:

1. using two independent sets of stress variables: the excess of total stress over the air pressure and the suction,
2. using one unified variable, the effective stress, which included in a single expression the effect of the total stress and the suction.

Alonso, Gens and Josa [3] wrote in 1990 probably the most cited paper all about the history of soils mechanics (more than 500 citations within Scopus). Their work aimed at the first of these two frameworks and it has been generally accepted that, as they proclaimed more than twenty years ago, that we need more than one stress variable to define the stress-strain behaviour of partially saturated soils. This paper, far from trying to contradict or demolish their acknowledged and accepted paper, was focused on the second of these frameworks trying to demonstrate if it was also possible to define unsaturated soil behaviour by only one variable.

1.2. THE EFFECTIVE STRESS PRINCIPLE

The effective stress (σ') acting on a soil calculated by two parameters, total stress or applied stress from the force or system of forces applied (σ) less the pore water pressure, or neutral pressure also called, (u) according to:

$$\sigma' = \sigma_v - u \quad (1)$$

Where, typically for simple examples (i.e. terrain without any external charge):

$$\sigma_v = H_{soil}\,\gamma_{soil} \quad (2)$$

$$u = H_w\,\gamma_w \quad (3)$$

Nevertheless, this is only a representative of a very particular case of saturated soils with incompressible grains and a pore space completely filled with incompressible fluid.

Currently, there are several studies where the aim is to model the behaviour of unsaturated soils (i.e. when a part of the pore volume is filled by air). In this condition, the state of tension is more difficult to estimate due to the interstitial water and the gaseous phase between the pores found in those conditions. This water acquires a suction, which reports some resistance, which is not contemptible at all, and this resistance is due to the capillary effect. This suction appears, in the case of a concave liquid bridge, because the gas pressure surpasses the liquid pressure surrounding the liquid bridge. Normally this pressure difference brings the grains closer (attracting actions, capillary and adsorption), which gives an additional resistance. Surface tension is also a determinant actor; the liquid-gas interface, which behaves like a tight membrane characterised by a surface tension standing in the way of any deformations.

Therefore, the capillary force due to the liquid bridge is measured as the sum of two terms; one related to the surface tension γ (direct effect) and the pressure difference Δu across the gas-liquid interface (indirect effect). The capillary force, graphically represented in Figure 4, is calculated at the apex following the “gorge method” [4]:

$$F_{cap} = 2\pi y_0 \gamma + \pi {y_0}^2 \Delta p \quad (4)$$

Where:

y_0 is half of the meniscus diameter when the spheres are in contact,
γ is the surface tension,
Δp is the difference in pressure.

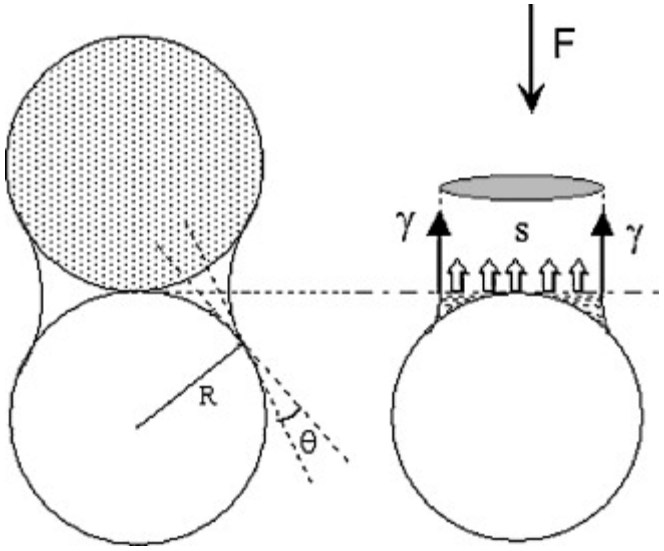

Figure 4: The capillary force illustrated from [5]

The volume of the non-saturated soil is modified as it is submitted to a differentiated tension state and influenced by a component denominated suction tension. The suction is able to vary the soil volume; nevertheless, its magnitude depends on the moisture of the porous medium, then, suction and moisture are closely related. In places where soil is partially saturated, traditional soil mechanics is not necessarily proper and can lead us to solutions with over-sized designs (for satisfying a critical condition) of really high cost and unrepresentative of the medium in which they find themselves.

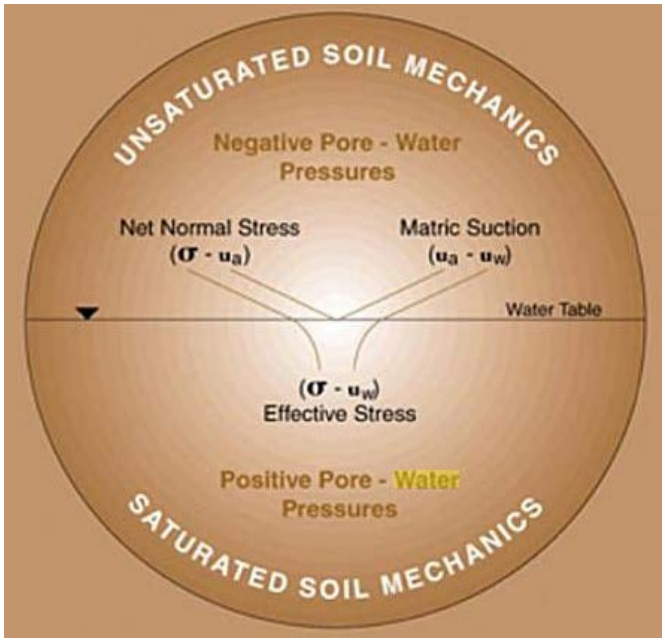

Figure 5: Diagram of the stresses and pressures suffered from Ref. [6]

1.3. EFFECTIVE STRESS PRINCIPLE WITHIN UNSATURATED SOIL

In determining the behaviour and strength of unsaturated soils, it became difficult to choose the controlling stress variable that would substitute for the role of effective stress in the saturated case. It was in trying to fix this shortcoming that Bishop (1959) extended Terzaghi's effective stress principle to account for the presence of an air phase by intuitively modifying the expression (1) and introducing an average pore fluid pressure weighted over the pore air (u_a) and water (u_w) pressures, i.e.

$$\sigma' = \sigma - [\chi u_w + (1-\chi)u_a] = (\sigma - u_a) + \chi(u_a - u_w) \quad (5)$$

Where σ and σ' are the total and effective stresses respectively, and χ is the weighted parameter that is arbitrarily confounded with the degree of saturation, Sr. This parameter is widely explained in the theoretical study of this paper. It is important to make quite that Bishop has never postulate that χ = Sr. He just said that χ is a function of Sr; it was much later when χ = Sr began to be used, because of the simplification that it means.

Bishop was not the only one who tried to get a more realistic and accurate distribution of the effective stress. In Table 1, we can see different approximations, introducing parameters to have the presence of water in account, and moreover its distribution, within the non-saturated granular media. This distribution could be very different depending on the state, as clearly displayed in Figures 5, 6, 7 and 8, giving more validity to various equations for a given state, but not for the others, being instable and unreliable as a practical tool. In fact, this issue is still the topic of large discussions and debates in the soil mechanics community. Thus, in order to contribute a little bit to this research we tried to obtain an effective stress deduced from the measurement of capillary forces between spherical particles by means of different procedures, which later were compared to each other, as well as with numerical simulations.

Within all these equations the expression by Bishop (1959) still attracts attention, formed in bygone days in an acceptable manner using the data available at the time. For that formulation, the parameter χ varies from 0 for dry soils, to 1 for saturated ones, and the intermediate values depend on the stress trajectory, on wetting and drying cycles, and mostly on degrees of saturation. Subsequently, experimental studies on the subject proved that the effective stress equation on unsaturated soils has limitations.

Jennings (1961), found that the Bishop's expression (1959) does not define the behaviour (relation between the voids rate and the effective stress) of most soils with a degree of saturation, below a certain critical value.

Bishop, with Blight, (1963) made some reflections about the first formulation in [7] and attributes that a suction variation does not correspond to an interstitial stress variation. Other authors questioned the formulation when the volumetric deformations or shear strength phenomenon were considered. Thus, the difficulty of obtaining the factor χ when it is associated with volumetric deformations is evident, because if effective stress goes down, either collapse or soil expansion could happen. This depends on the term of the equation that is reduced. If it is only suction that is reduced, a collapse may occur. If the fall is within the overall stress, the expansion of the soil as observed by Alonso and Lloret in 1985 may happen [8]. It is important to remember that

under elasto-plasticity conditions strain is no more directly proportional to the stress, meaning that the effective stress principle is not able to reproduce the collapse.

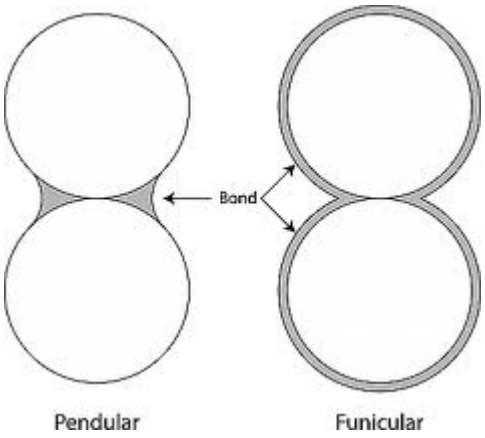

Figure 6: Water distribution in different states

Faced with the difficulty of quantifying the value of the parameter χ, Aitchison (1961), considered that, given the variability of this parameter, it was only possible to obtain an appropriate value of effective stress considering a single path for each term of σ' and $(u_a - u_w)$, reasoning that makes it unnecessary to quantify χ. Due to the already presented difficulties in quantifying the effective stresses introducing an independent unitary parameter, the evaluation of soil properties as volumetric change and soil strength were performed using the concept of state variables, described by Matyas and Radhakrishna (1968) in [9].

Equation	Reference
$\sigma'=\sigma-u_a+\chi\,(u_a-u_w)$	Bishop (1959)
$\sigma'=\sigma+p''$	Donald (1956)
$\sigma'=\sigma-\beta'.u_w$	Croney, Coleman & Black (1958)
$\sigma'=\sigma+\Phi.p''$	Aitchison (1961)
$\sigma'=\sigma+\beta p''$	Jennings (1961)
$\sigma'=\sigma-u_a+\chi_m(h_m+u_a)+\chi_s(h_s+u_a)$	Richards (1966)
$\sigma'=\sigma-u_a+\chi_m.p''_m+\chi_s.p''_s$	Aitchison (1973)
$\sigma'=\sigma-u_w.Sr-(1-Sr).u_a$	Öberg & Sällfors (1997)

Table 1: Different approximations for effective stress in non-saturated soils, extracted from [10]

Where:

χ: parameter related with the saturation degree;

u_a, u_w: air and water pressure respectively;

p": water pressure below atmospheric pressure;

β´: union factor;

Φ: parameter between 0 and 1;

β: statistic factor for measuring contact area;

χ_m, χ_s: parameters of effective stress for matrix suction and of solute respectively;

h_m, h_s: matrix suction and solute respectively;

$p"_m$, $p"_s$: matrix suction and solute respectively;

Sr: Degree of saturation.

Consequently, although there were several approximations, we concluded that effective stress in unsaturated soils was never physically or mathematically defined. None of these approximations showed the behaviour of all ranges of the degree of saturation, being the first one; only acceptable within the pendular state.

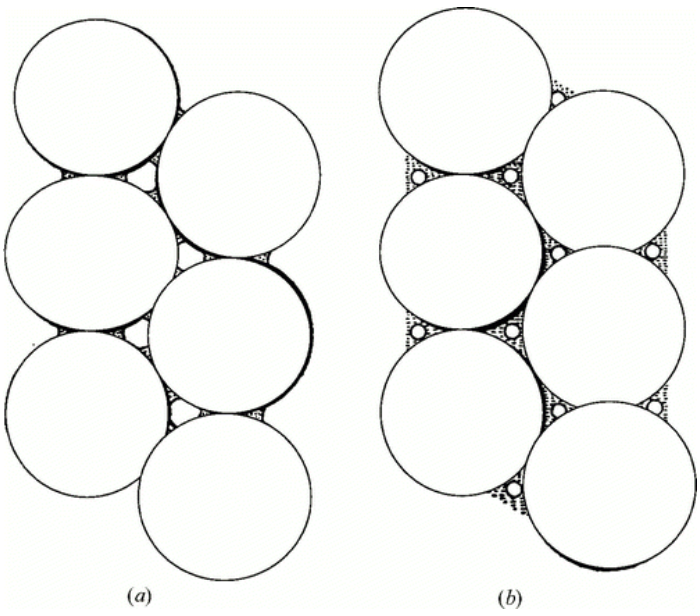

Figure 7: Comparison between pendular (a) and a funicular state (b) from Ref. [11]

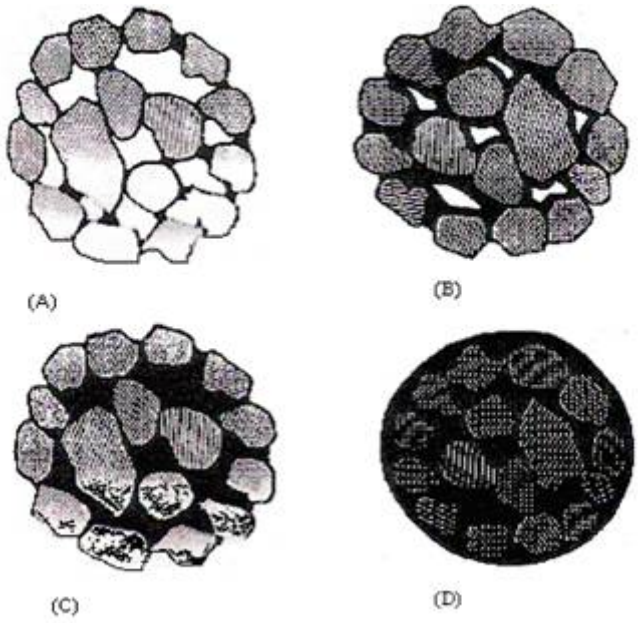

Figure 8: States of saturation in a spherical assembly of particles: (A) pendular state, (B) funicular state, (C) capillary state and (D) droplet state from [12]

SATURATION DEGREE [%]	SATURATION REGIME		MEAN FORCES
0 %	Dry	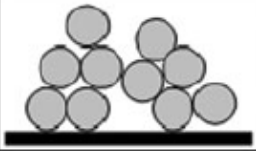	Gravity, contact
0% - 5%	Pendular	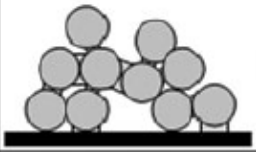	Gravity, contact, capillary
5% - 35%	Funicular	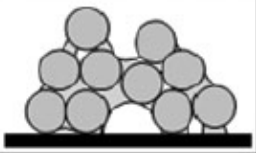	Gravity, contact, capillary
35%-90%	Capillary	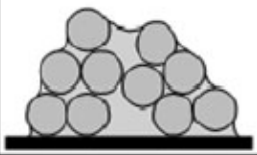	Gravity, contact, capillary, [drag]
90%-100%	Saturated	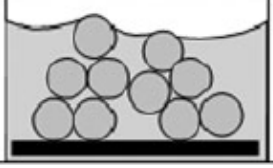	Gravity, contact, [drag]

Table 2: Soil saturation states from [13]

1.4. SUCTION

Suction in unsaturated soils is compounded by matrix suction (S_m) and osmotic suction (S_{osm}) and the sum of both components is called total suction (S_t). In that context, the magnitude of the total suction corresponds to the overall work done by the capillary force, absorption and the osmosis. The total suction is represented in pressure units and this can be expressed as follows:

$$S_t = S_m + S_{osm} \quad (6)$$

The total suction is defined as the negative gauge pressure, related to the external pressure of the gas over the water, which will should be applied to a reservoir of pure water (at the same level and temperature) in such a way that it stays balanced, through a semi-permeable membrane (enabling the water flow but not the solute's), between the water reservoir and that of the soil. Figure 8 illustrates the concepts of matrix, osmotic and total suctions.

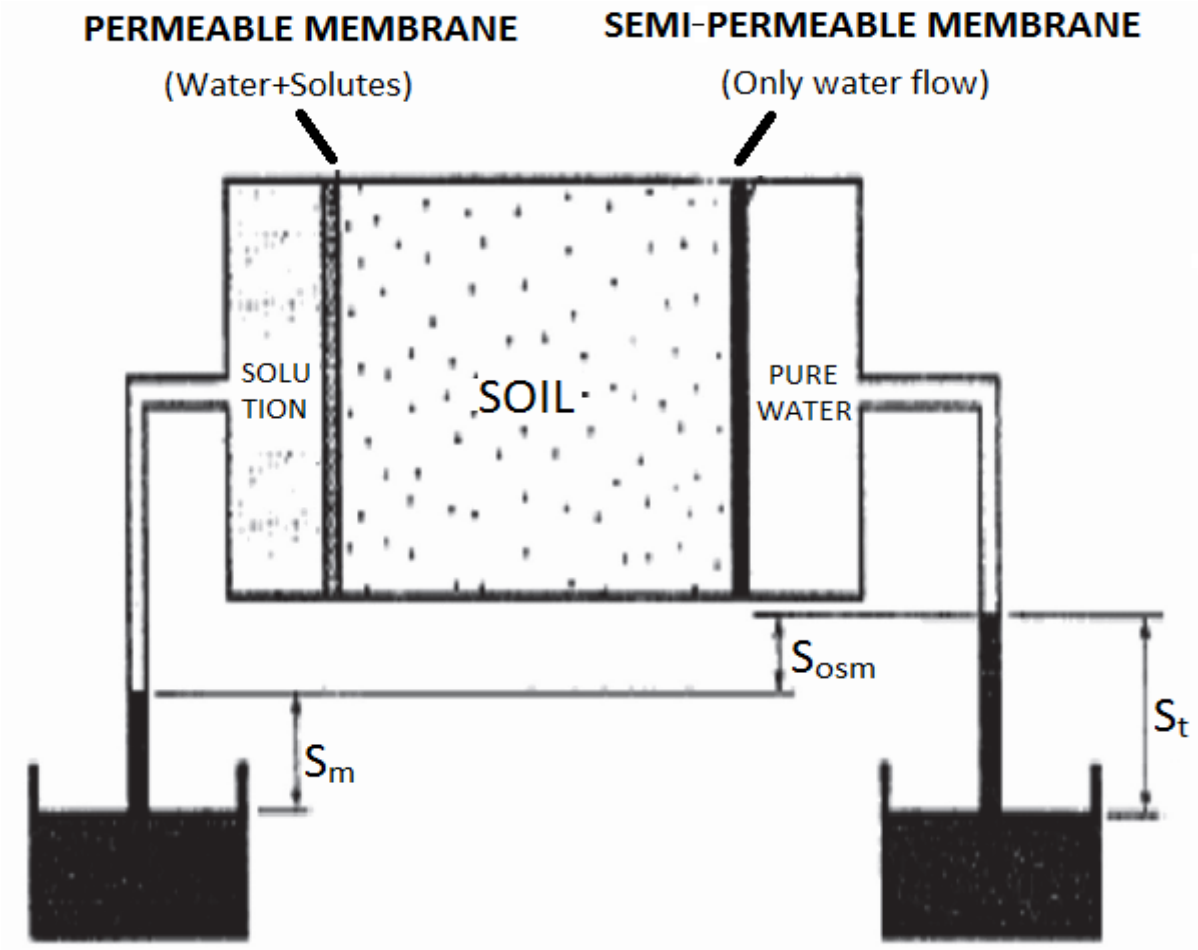

Figure 9: Representation of the concepts of matrix, osmotic and total suctions from [7]

Matrix suction (S_m) is equal to the total suction when the soil water is identical to the standardised water (pure water or solution with the same composition of the soil water), hardly leaving the effect of the soil matrix (capillarity and absorption). The matrix effects come from the developed pressures of the capillary meniscus and water absorption due to forces exerted by the particles surface. These are globally quantified because of the difficulty of discriminating them as explained in Ref. [14].

Osmotic suction (S_{osm}) is equal to the total suction when the soil is saturated, meaning that, when the matrix component does not take place, having only the effect of the solutes concentration. In Figure 9, the water is pure and is in contact with soil (with higher solutes concentration) through a semi-permeable membrane which is permeable to water molecules and not for solutes.

The importance of the osmotic suction in Soil Mechanics seemed to be more related with the dispersive or expansive soils, even admitting that the value of the total suction corresponded almost entirely to matrix suction [15]. Consequently, in practice, it is usual to consider the suction of the soil as the matrix suction. Nevertheless, to not have to make extra considerations, distilled water was used, to avoid the apparition of osmotic suction.

1.5. SUCTION VS. MOISTURE

The ratio of suction (total, matrix or osmotic) versus moisture (degree of saturation, volumetric moisture or gravimetric), was important for the characterisation of unsaturated soils. The graphical representation of this ratio is so-called "soil-water retention curve" (SWRC) [16].

According to Fredlund and Al. [17], the soil water retention curve can be defined as the variation of the suction capacity of retaining water in the macro and micro soil pores. The values correspond to the kind of soil, with a given density and, generally speaking, the pores geometry, the magnitude and the mineralogical composition of this fine fraction are crucial to the relative position, the shape and the slope of the curve.

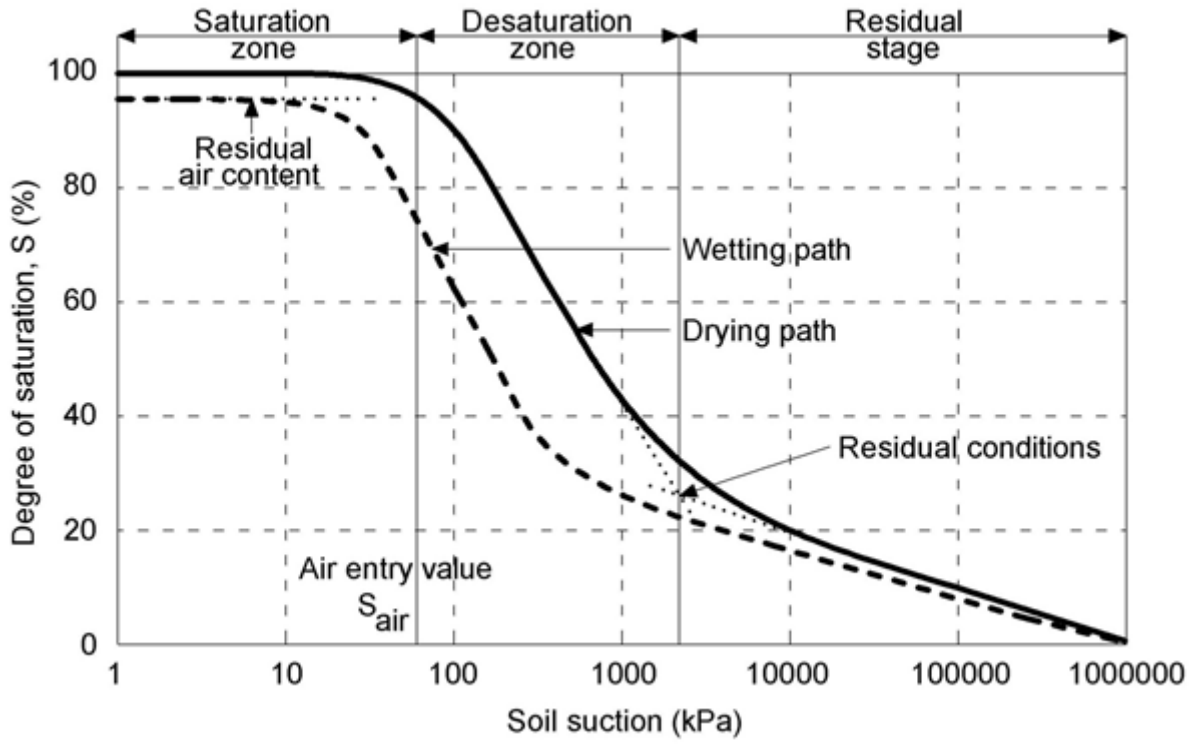

Figure 10: Typical soil-water retention curve from Ref. [18]

The retention curve can be characterised with the purpose of equating it. The characterisation is done from the typical trajectories obtained by drying or wetting processes. Figure 10 shows the characteristics of the retention curve, obtained by drying and wetting, being clear of the hysteresis phenomenon (curves mismatched by both processes) associated to the two procedures.

Something that is well known and a common point for all in the scientific community is that capillarity phenomenon has an important place within the mechanical behaviour of unsaturated granular soils, and it deserves to be well-studied. What makes the study of this media even more difficult is the fact that the water takes a different shape depending on the state of the soil. Since a clear quantitative categorisation in terms of saturation degree or water content is impossible, as the transition from one state to another state depends on the physical and geometrical properties of the grains (solid nature, grain size, shape, density) and liquid properties, the value of saturation degree reported in Table 2, must be considered as purely suggestive.

As indicated in Table 2 [13], the water saturation in soils may be divided into the following five states [19]:

- Completely dry, when water content is zero,
- Pendular state, when the air domain is connected and a little amount of water is shared by couples of grains forming the so-called capillary bridge or pendular ring or meniscus,
- Funicular state, when pendular rings collapse on one another and the water is shared by three or more solid grains,
- Capillary state, when the liquid domain is connected and air is confined in some bubbles,
- Completely wet or saturated, when the air content is zero.

1.6. GEOMETRY AND SURFACE EFFECTS

The shape of the particles and their relative position can bring a type of “apparent cohesion” within the granular media without having a physical or chemical attraction between particles. This kind of cohesion is described as “apparent” as strictly speaking it does not comprise of cohesive actions between grains, but we observe a resistance in the relative displacement of the grains, which certainly has elements in accordance with cohesion.

The particles’ geometry of contact surfaces and surface irregularities can create obstructions and therefore a resistance displacement in one direction, which contributes to the global cohesion, restricting the movement of contact particles. In fact, this certain roughness is able to modify the capillary force [20]:

- The ruggedness regime (Fig. 11a) appears when weak quantities of liquid are in the media. The capillary mechanism is held in place by the liquid accumulation around a small number of asperities in contact. This regime stands as long as the region wetted by the liquid bridge does not exceed the distance between the two irregularities (ridges or grooves).

- When the amount of liquid increases, a lateral extension of the liquid bridges occurs and the roughness regime is attached (Fig. 11b). The meniscuses grow, filling some microgrooves with liquid.
- When the lateral extension of the whole liquid between grains is stabilised, the average radius of curvature of the grains becomes dominant compared to the characteristic sizes of the asperities, the spherical regime is reached (Fig. 11c). Within this regime, the roughness has a weak influence onto the capillary force and it can be studied with the assumption of smooth surfaces, so its effect is contemptible.

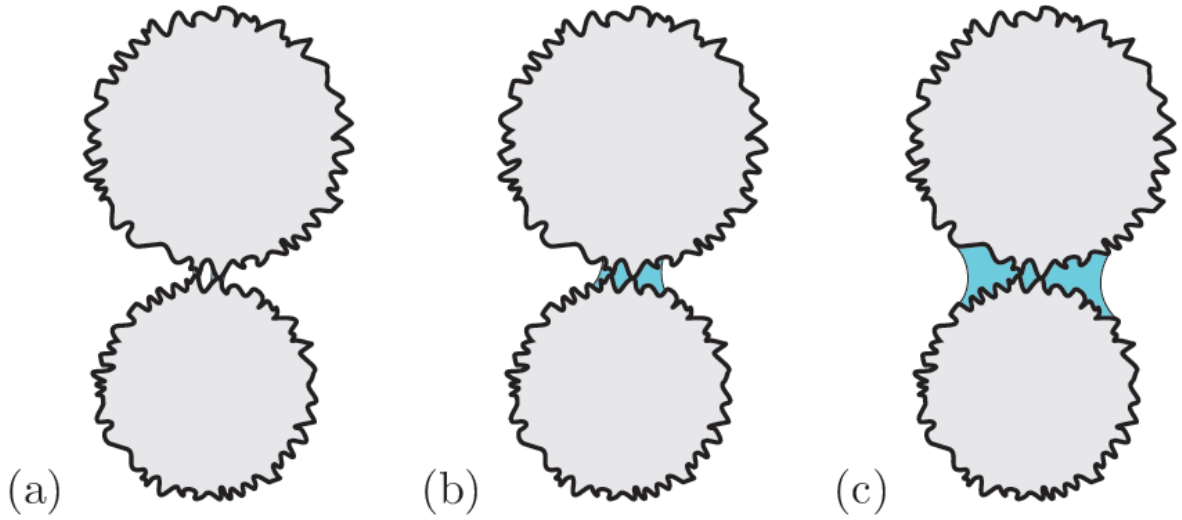

Figure 11: Capillarity and roughness: (a) ruggedness regime, (b) roughness regime and (c) spherical regime from [21]

1.7. SHEAR STRENGTH

The water presence within the granular media produces cohesive action, but can also modify the friction between grains. Due to this, a second series of micro-mechanical tests were initially contemplated (and finally rejected, as later explained) in order to measure the shear strength between particles linked by water meniscus. Some numerical triaxial tests done in Ref. [22] with different water contents and confinement stresses were performed: the analyses permitted to emphasise the shear strength increase occurring at low water content.

As thoroughly explained in Ref. [23] it is well known that in many circumstances the natural slopes of granular material may exceed their specific soil friction angle for no apparent reason. This behaviour is due to the presence of an apparent or real cohesion among soil grains, which may be caused by several physical and chemical phenomena. For example, in volcanic soils, it is common to observe a weak mineral binder between grains capable of producing slope angles greater than 40-50°, while remoulded soil has friction angles typically ranging from 20 to 30° [24]. Other materials, like some cemented sands, sandstones and clastic rocks, show similar behaviour because a partial

mineral cementation present at the inter-particle contacts, provide a global tensile strength [25] and this mineral bond can support tangential forces unlike the liquid bond in partially wet sands.

Although the inter-particle force intensity may vary to several orders of magnitude, tensile stress may be easily experimented similarly in all partially wet granular soil, especially in fine-grained ones: this is a well-known feature of sand as demonstrated in its wonderful capacity for building sandcastles [26].

The phenomenological mechanical behaviour of any soil in a partially saturated condition is, at first sight, non-trivial to be analysed because solid grains, water and gas have very different rheological and physical properties and no homogenisation or mixture theory may be easily adopted. Every phase interacts on various levels: in purely mechanical, thermodynamically and more generally energetic ways.

Moreover, the response in shear strain conditions to dry and wet granular materials is nonlinear, due to the dissipative mechanisms – i.e. the mutual slip at contacts and rotation of grains – that are mainly controlled by the solid phase, especially in quasi-static conditions.

Indeed, granular materials have the same strength in completely saturated and dry conditions whilst in pendular and funicular states the liquid tension may highly modify the shear strength.

2. EXPERIMENTAL STUDY

2.1. MICRO-SCALE EXPERIMENTS

2.1.1. TRACTION EXPERIMENTS

2.1.1.1. TEST BED

The need for a test bed can be justified by several reasons: the main one is probably the need for an experimental validation of the below described simulation, and the theoretical approximations. Moreover, the inherent assumptions of the built model prevent us from getting results from nonaxially symmetric configurations. A test bed can then feed us with additional information such as, for example, the influence of the gripper tilt on the capillary forces. A third reason is that the simulation has to be fed with input data such as the amount of liquid and the contact angles: these inputs will be measured with this test bed. Moreover, it is still not clear which contact angle (advancing vs. receding one) should be used: the choice will be achieved by direct observation of the picking operation.

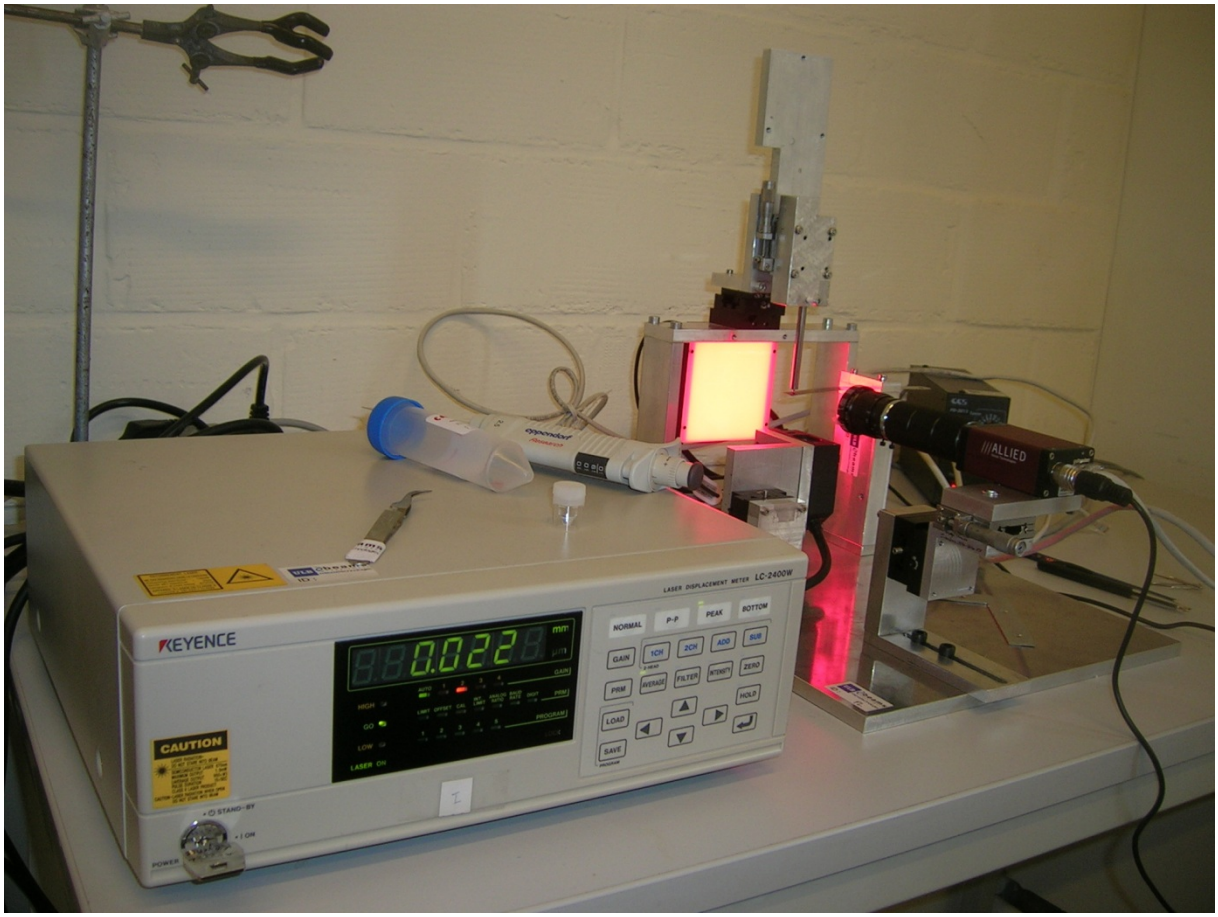

Picture 1: Micromechanical test bed

2.1.1.1.1. FORCE MEASUREMENT

The variation of the deflection of the beam was measured by a noncontact displacement sensor. This variation, together with the stiffness of the cantilevered beam, gives the amount of force applied onto this beam. This force is exerted by a meniscus that has been dispensed between the ball glued onto the beam, which acted as a component, and the upper solid, another ball, which acted as a gripper.

According to Ref. [27], the sensing of small forces can be achieved by measuring the displacement caused by elastic deformation induced by the loading of an elastic structure. However according to the reference, there are many usual deformable sampling bodies, but the most suitable body is the cantilevered beam (Figure 12) as it can serve both as deformable body for the force sensing and as a component for the experiment. If the component material has to be changed, another blade can be used or a small flat sample can be glued onto it.

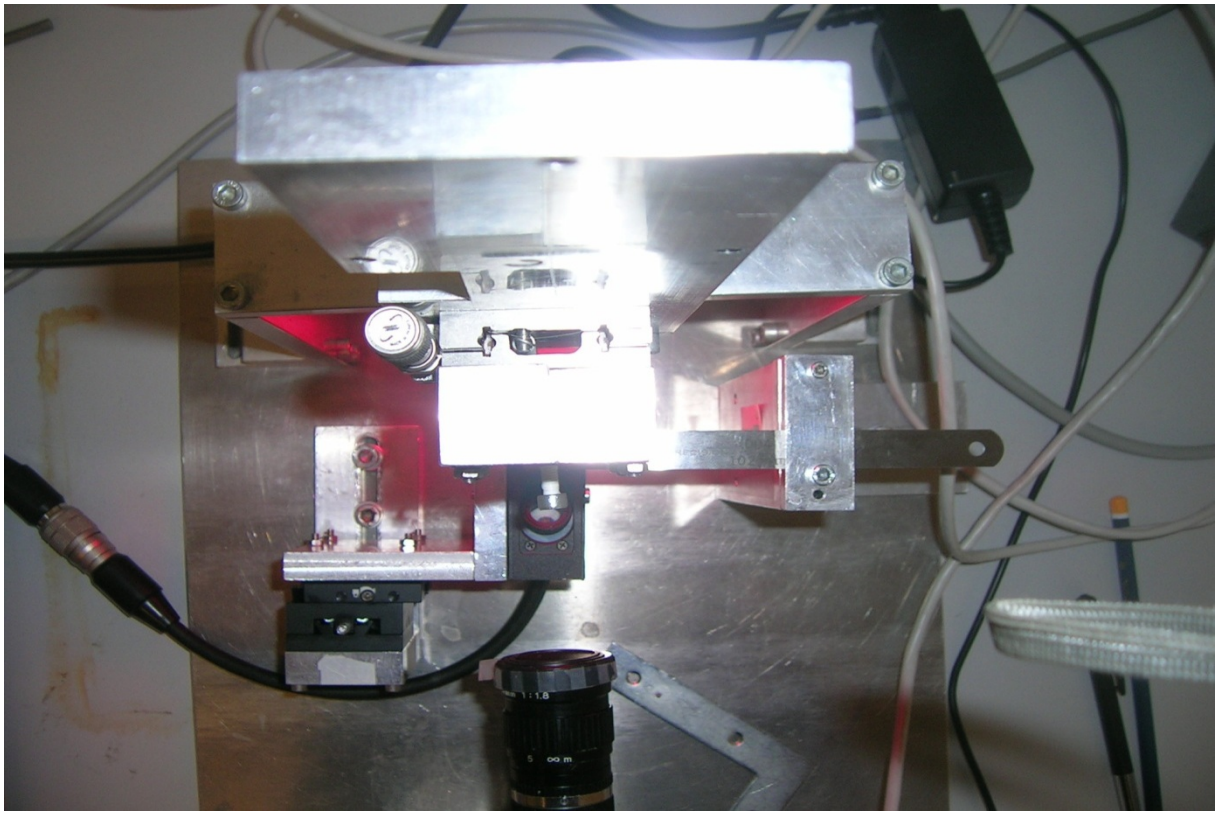

Picture 2: Experimental set up, view from above

Because of its small thickness, the blade extremity undergoes a deflection δ_{weight} due to its own weight:

$$\delta\text{weight} = \frac{qL^4}{8EI} = \frac{3}{2}\frac{\rho g}{E}\frac{L^4}{\text{h}^2}. \quad (7)$$

Where L is the length of the beam (m), q is the distributed load per unit length (N m^{-1}), i.e., q = $\rho g \text{h} b$, where ρ is the density of the beam (kg m^{-3}), g is the well-known gravity constant (9.81 m s^{-2}), h is the beam thickness (m), and b is the beam width (m). E denotes the Young modulus of the material (Pa)

and I refers to the momentum of the beam section, i.e., $I = b\mathrm{h}^3/12$ (m^4). Typical values are given in Table 3 and 4 for our using material, the plastic Polyethylene terephthalate.

Note that this deflection does not actually disturb the measurement as deflections are assumed to be small. Consequently, the linearity and the superposition principle can be applied and the own deflection is neglected.

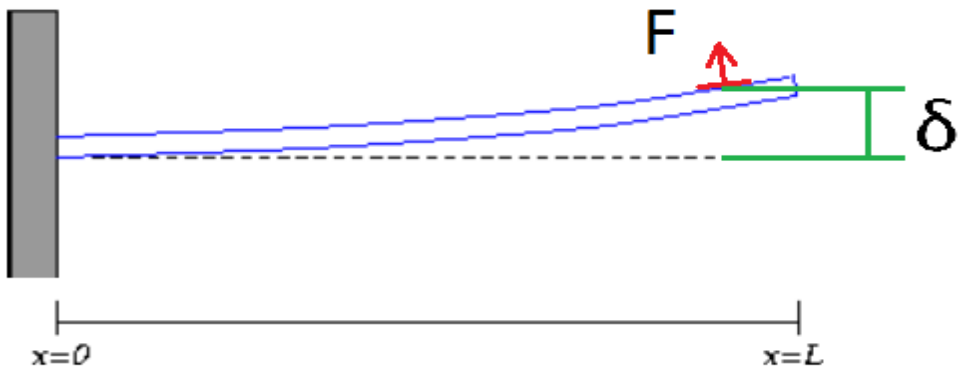

Figure 12: Chosen force sensing principle on a cantilevered beam

Table 3: Geometrical properties of the cantilevered blades:

Symbol	Description	Value	Units
L	Length	10-100	10^{-3} m
h	Thickness	0,025-1	10^{-3} m
b	Width	12	10^{-3} m

Table 4: Physical properties of the cantilevered beam:

Symbol	Description	Plastic	Units
E	Young's modulus	2.3	10^9 Pa
ρ	Density	1,400	kg m^{-3}

In (7), the δ_{weight} currently cannot be directly reduced because it would imply a loss of sensitivity as far as the force measure is concerned. Indeed, the deflection δ_{force} caused by an external load F (expressed in N) is given in [28]:

$$\delta\mathrm{force} = \frac{FL^3}{3EI} = \frac{4FL^3}{\mathrm{Ebh}^3}. \quad (8)$$

Consequently, we should try to maximise the following M ratio, describing the relative importance due to force deflection compared to weight deflection:

$$M = \frac{\delta\mathrm{force}}{\delta\mathrm{weight}} = \frac{8F}{3\rho g b}\frac{1}{hL}. \quad (9)$$

If the density of the cantilevered and its width are fixed, we have the following two considerations for a given force:

1. The thickness h and the length L should be as small as possible in order to reduce the relative importance of the weight
2. h should be as small as possible in order to maximise the sensitivity of force measurement, but the length L should be maximised.

We concluded that the thinnest cantilevered beam should be chosen, as its length is adapted for minimal sensitivity. At first the beam was made from steel, but we began to obtain strange results; it was like the experiment was against the physics, as we know it, because we was obtaining a much higher normal force without water, than with it. After lots of hours of desperation and reflexion (and a little bit of help) we realised that it was all magnetised. We could have tried to demagnetise the beam with a turbine (all the test bed would be much more difficult) and tried to see if that was sufficient or change the material, which in the end was my decision. Between all the different thicknesses we could have chosen, we used that one with similar characteristics to the steel one, according to the criterion explained above.

In addition, we obtained another approximation, giving results of the same magnitude as the preceding formula, this time using the deflection values from the plastic beam produced by moving one particle away from the other, displacing the 1D manual stages used on the experimental arrangement. The following formula was used:

$$F_{cap} = \delta k \tag{10}$$

Where:

δ is the deflection measurement

k is the stiffness of the plastic beam, calculated by measuring the deflection of the beam with three weight-known small objects, placed around the glued ball. In Figure 13 we can see the linearity of the system, which proves the quality of the measurement system. The obtained value is k = 1.5 N/m and it is easily noticeable in the picture.

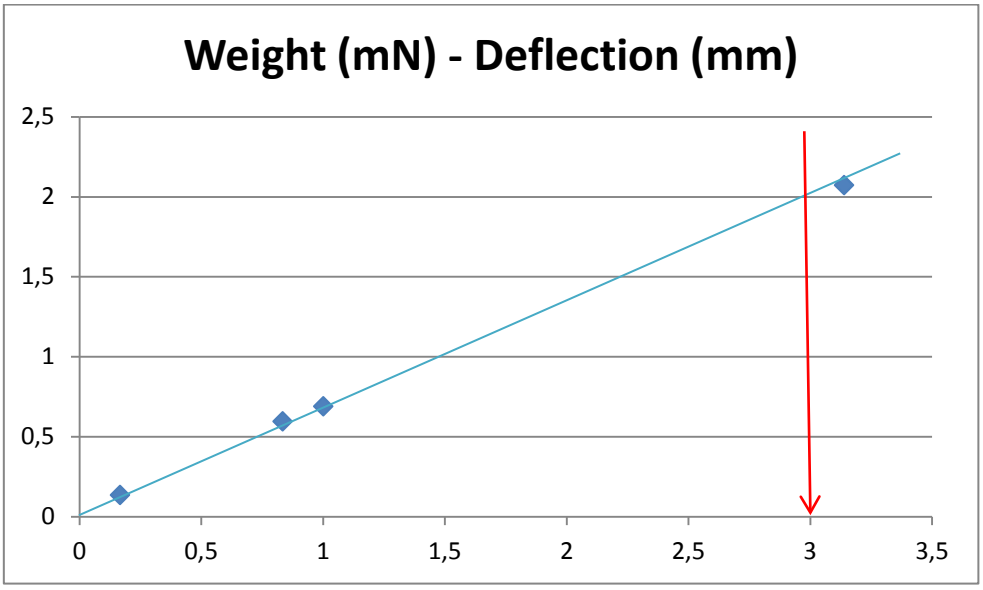

Figure 13: Different deflections of the four masses, used to calculate the stiffness of the plastic beam

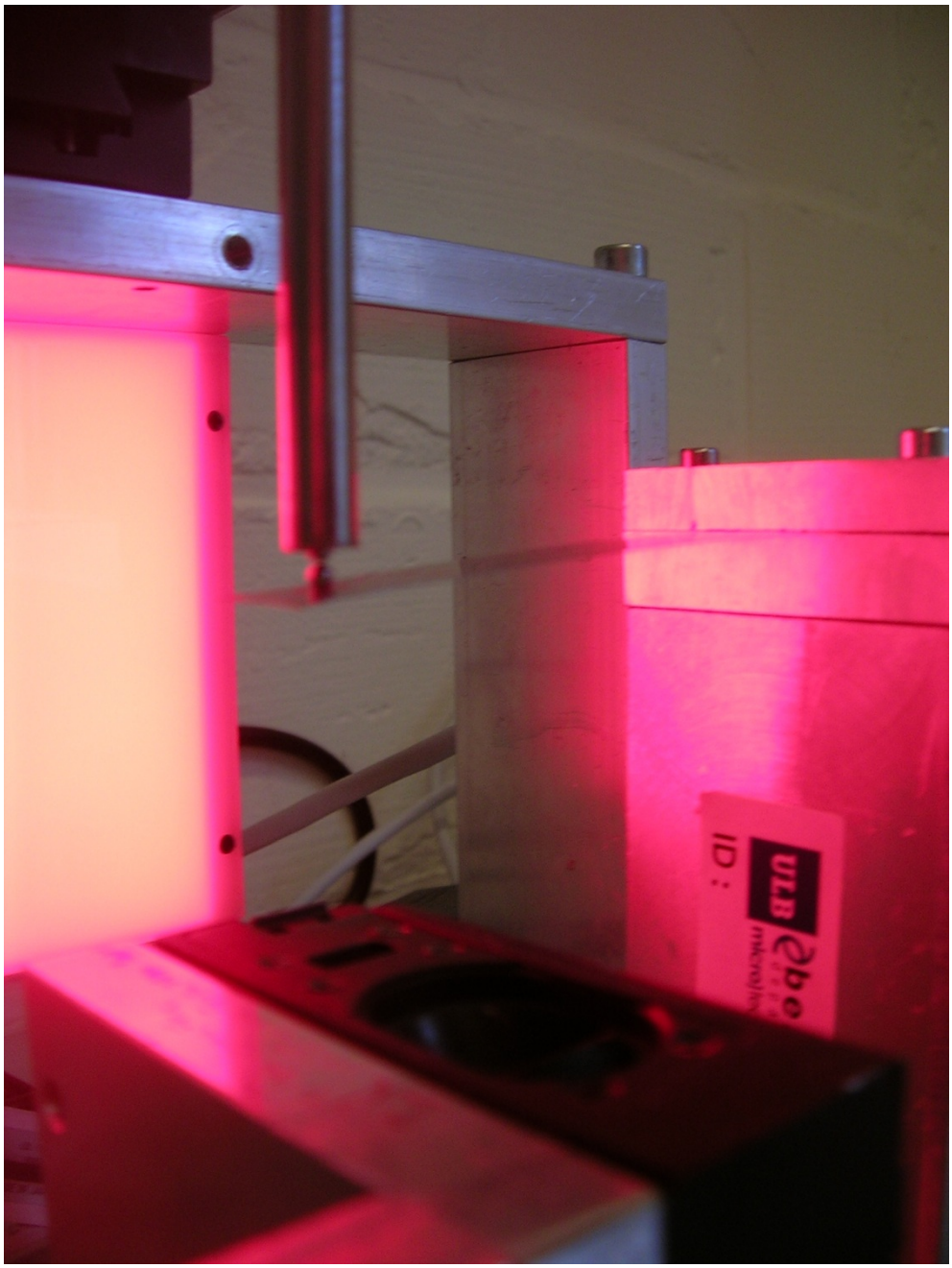

Picture 3: Detailed view of the beam, the balls and the gripper

The deflection measuring system was implemented as follows: at equilibrium the capillarity upward force F exerted by the liquid bridge on a cantilevered beam was balanced by the elastic restoring force due to the beam deflection δ (Fig. 12). This deflection was directly measured by a noncontact displacement sensor (Keyence LC-2440 laser), of which the measuring range is equal to 3 mm and accuracy is guaranteed by the constructor (see Annex 3) to be 0.2 µm. The measured value can be read immediately on the controller display or can be transmitted by a RS-232 connection in order to achieve almost real time acquisition.

2.1.1.1.2. DROP DISPENSING

For these experimental tests, a manual dispensing system was used. Since the liquid amount was an input parameter of the simulation tool, it had to be done with accuracy. It is either calibrated with the manual dispensing device (from 0.1 to 2.5 µL, with steps equal to 2 nL) or it can be measured from the height h and the diameter D of the droplet, normally going up from 576 to 1,684 µm [1]. This second method is not suitable for very small contact angles, because height h is too small to be measured accurately by number of pixels.

Picture 4: Manual drop dispensing

2.1.1.1.3. VISION

The camera used was the Keyence-CV050 CCD camera, mounted with a 50mm lens and a set of rings to tune the zoom; composed of two bracings each one at 45mm. The distance between the lens and the spherical tip was 44 mm.

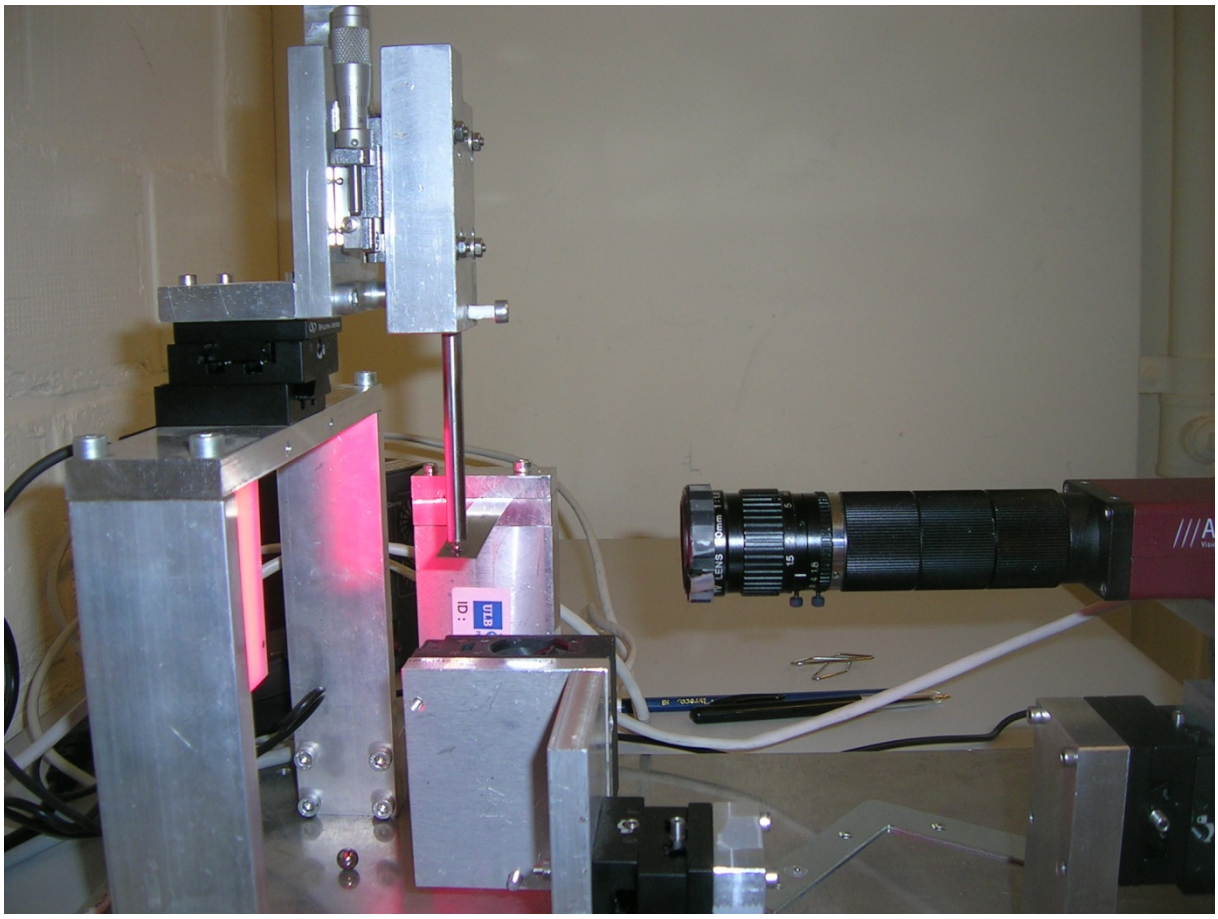

Picture 5: Experimental set up, side view

This device was coupled to a monitor in order to track the picture, to achieve several measurements (contact angle measurement, gripper geometry, volume of liquid), and to transfer the acquired image to the work station. The program used for that was GigEViewer. For the image treatment (measuring of angles and distances) ImageJ was used, a program easily downloadable from the Internet. For imaging droplets, a backlight illumination system was used.

2.1.1.2. MODUS OPERANDI

1) The gripper and the beam are chosen and set up: a small flat component made of steel was glued onto this beam, in order to simulate the desired material. Note that this operation does not disturb the force measurement as the weight of the additional component is quite small.
2) The force measurement system is calibrated by measuring the deflection corresponding to a known force, i.e., the weight of several reference masses placed onto the beam, around the ball.
3) The gripper is moved downwards until contact with the beam is detected.
4) Displacement sensors are set to zero.
5) The gripper is moved upwards to free space between its tip and the beam. A liquid droplet is then put on the beam right below the gripper tip; it is possible to know the volume by:
   a) Using the calibrated indication on the micro-pipetting device, and then supposing constant evaporation (realistic assumption checked by image analysis), which means that there needs

to be repetition of the process each x seconds, attempting for x to be as stable as possible, using the aid of a chronometer.

b) Computing the volume from the geometrical parameters from the spherical cap-shaped droplet.

c) Superposing the meniscus profile and the computed shape for a given input volume. If the shapes correspond with one another, then the volumes are equal.

Procedure a) was chosen because of its simplicity.

6) The gripper is moved downwards until the droplet turns itself into a liquid bridge. From this situation, the advancing (receding) contact angles are obtained by slowly moving the gripper downwards (upwards) and then directly measured on the camera monitor screen (Pictures 6 and 7). When taking a photo we applied a weak prestress, deflecting the beam -0.05 mm, to simulate a contact situation such as that the soil is found in.

7) Force measurement: The separation distance can be turned by moving the gripper. The cantilever deflection sensor should now display a positive value as the cantilevered blade is pulled upwards by the meniscus.

a) On contact, the force can be measured by the maximum deflection of the beam. Note that this maximum deflection can be difficult to read as this configuration is unstable: Indeed, from the maximal deflection situation, the beam quickly jumps downwards when the gripper height increases. The reason therefore is that the capillary force becomes lower than the elastic restoring force of the beam, and consequently, there is a jump from this position to a lower one, corresponding to another force balance, introduced by a larger gap. According to the stiffness of the beam, this second equilibrium position may or may not exist (this phenomenon is widely described in [29].

b) The force-distance curve can be drawn by moving the gripper downwards step by step until there is a physical contact between the gripper and the cantilever: during this phase, the deflection of the cantilever gives the value of the pulling force exerted by the meniscus.

Note that in step 5; at times it is necessary to calibrate the camera: this is achieved by imaging a ceramic slip gauge with a given width. In the case of study, we already know the diameter of the ball, so this procedure is not necessary. All the measurements needed for the different approximations were achieved using the ImageJ programme, and by making a conversion to mm by multiplying the obtained distance by 0.002, and dividing by 405, as each ball, had a real diameter of 2mm, it was then measured by the programme being 405 units.

We can therefore conclude that the scale is about 405 ± 2 pixel mm^{-1}.

2.1.1.3. CONTACT ANGLE

As the contact angles constitute inputs for the simulation, it was necessary to measure them. One way was to assume that a small droplet posed on a substrate would take a spherical cap shape; the contact angle θ was consequently able to be deduced from the drop height h and the drop diameter D, measured on the screen of the CCD camera controller. Unfortunately, as already mentioned in Ref. [1], this method does not work when θ is small because in this case it is difficult to determine the h, accurately, and when the hysteresis is large, due to the fact that it is difficult to

know whether the angle made by the spherical cap tends to be or not, the advancing or receding contact angles. Consequently, the final method consisted of transforming the droplet to a meniscus by putting the gripper closer to the blade at the top where the drop was posed. Once the meniscus had formed, the gripper moved slightly downwards (upwards) to force the contact line to move along the solids: in this case we were assured to measure the advancing (receding) contact angle as depicted in Figure 14.

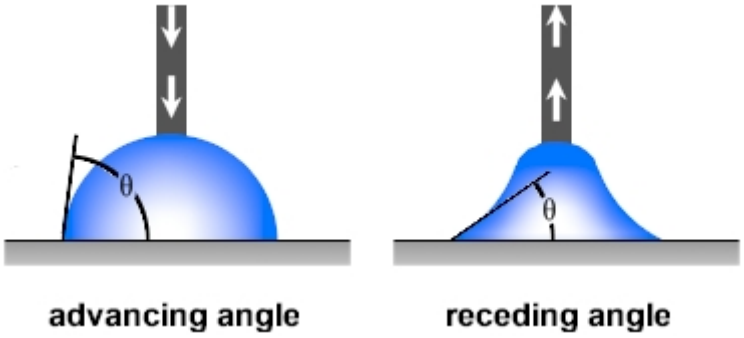

Figure 14: This diagram illustrates the formation and measurement of an advancing and receding angle using the volumetric expansion and contraction method from [30]

Picture 6: Advancing angle

The performance was the following:

We took a photo of each angle (advancing and receding) in a serial of 5 experiments. Meaning that the quantity of water was supposed to be the same each time, because we used a manual dispensing system, which gave 0.6 µl of liquid, and the surface of the balls was cleaned properly each time, to assure that there was not any stocked water when we began the next experience.

Once the drop was placed between the two balls, we brought the balls closer together, until the wet surface began to rapidly increase, when we stopped and took a photo. Then, we moved the balls away until the wet surface began to decrease rapidly, which is when we stopped the manipulation and took another photo. This therefore shows the procedure used to experimentally obtain the advancing and receding angle, obtaining the contact angle with their subtraction. The hysteresis phenomenon is well known, and this makes the determination of the contact angle complicated.

Picture 7: Receding angle

At first sight the upward motion of the gripper during the picking step seemed to lead to a receding motion of the liquid and consequently to a receding angle, as displayed on the second image of the Figure 14. However, coming into closer contact with the component, the approaching motion of the gripper pushed the liquid outwards, with an advancing contact angle (first image of

Figure 14). In the beginning the upward motion of the gripper the angle was still the advancing one because the gripper (and consequently the liquid too) had not yet begun to move. It was only when the gap began to increase that the contact angles moved from advancing to receding ones. This assumption was validated by direct observation of the scene using the CCD camera. The angle θ was measured 5 times in picking situation, leading to the following (average) result: $\theta_{rec} \approx 39°$, and the same for the approaching motion, which produced an angle of: $\theta_{adv} \approx 63°$; all angles had to be compared with those of Table 5.

Table 5: Measured contact angles of the steel-water combination by [1]:

Solid-Liquid combination	Advancing	Receding
Steel-Water	88°	37°
cos θ	0,034899497	0,79863551
$F = 4\pi\gamma R\cos\theta$	3,19052E-05 mN	0,000730115 mN

It was measured the average of the contact angle in every configuration, i.e. with all the different volumes of water stocked between the balls. In Figure 15, we can see the decreasing contact angle that we have when losing water, going from the spectrum of contact angles ranging from the so-called advancing (maximal) contact angle to the receding (minimal) contact angle.

Table 6: Measured contact angles, showing a high dispersion and hysteresis:

	Photo 1	Photo 4	Photo 5	Photo 3	Photo 2
Advancing	45,2275	74,5125	83,6525	56,825	53,0175
Receding	29,735	38,7325	42,31	39,275	42,6925
Mean	37,48125	56,6225	62,98125	48,05	47,855

As calculated before for the pair contact of particles, the degree of saturation, Sr, was obtained for all the different quantities of stocked water, as the division of the water volume at any time, divided by the pore volume, which was continually constant.

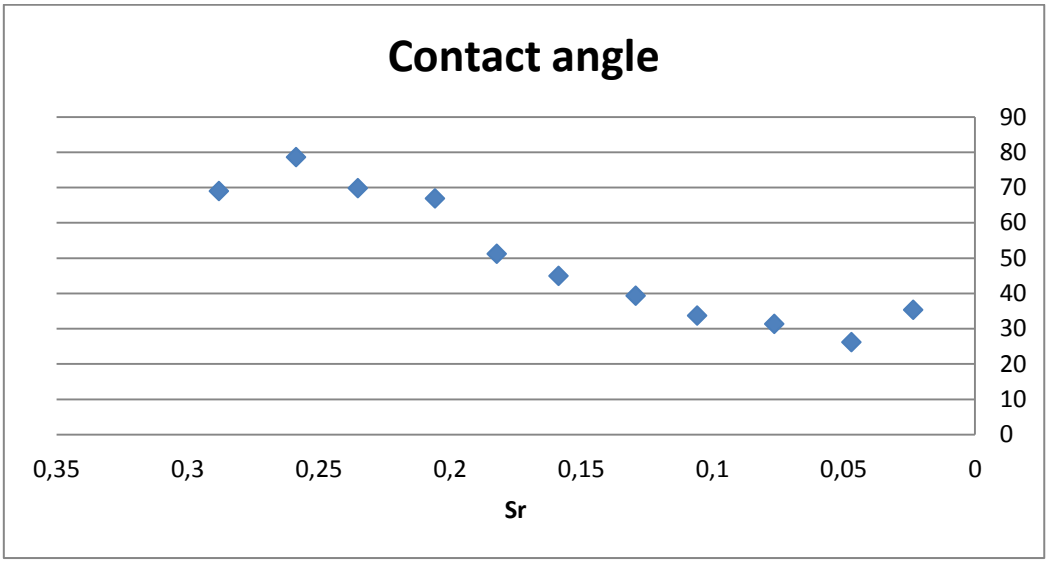

Figure 15: Evolution of the contact angle with the decreasing degree of saturation, obtained by photography manipulation

2.1.1.4. FILLING ANGLE

The maximum degree of saturation is reached whenever the filling angle reaches its maximum and the curvature of the meniscus decreases to a minimum so that the toroid degenerates into a cylinder. As we can see in Figure 16, the filling angle always increases with the degree of saturation. With these angles, we have obtained both, λ_1 and λ_2, parameters needed for the obtaining of the effective stress parameter χ.

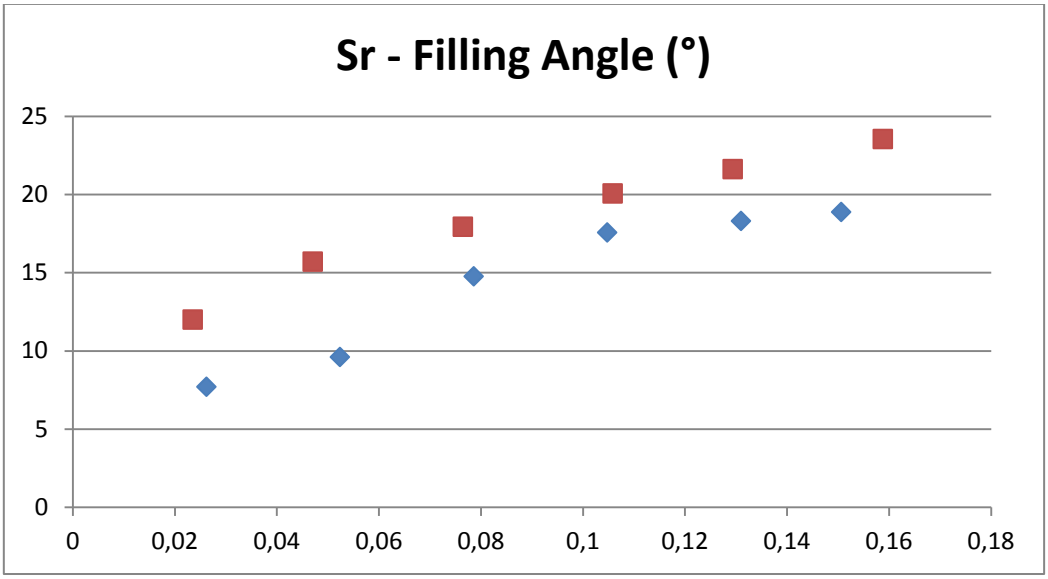

Figure 16: Evolution of the filling angle whilst the degree of saturation is increasing, obtained by photographs taken in two series' of micromechanical experiments consisting of two pairs of balls in contact with a decreasing content of water due to evaporation, assumed as constant

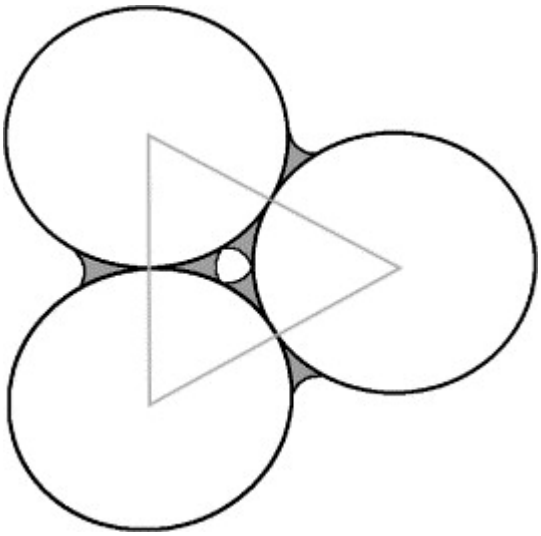

Figure 17: Geometrical demonstration of the affirmation on the maximum filling angle for avoiding coalescence, which is no other than 30°

To determine the filling angle we measured the four angles in each picture with the different volumes of water. As we can observe in Figure 16, there is no angle superior to 30°, (which was our proposal, according to the logic in Figure 17) putting the amount of water at (0.6µl) and not more, to fundamentally avoid the coalescence as depicted in Figure 18, which forms a big meniscus, containing some balls and a meniscus between them.

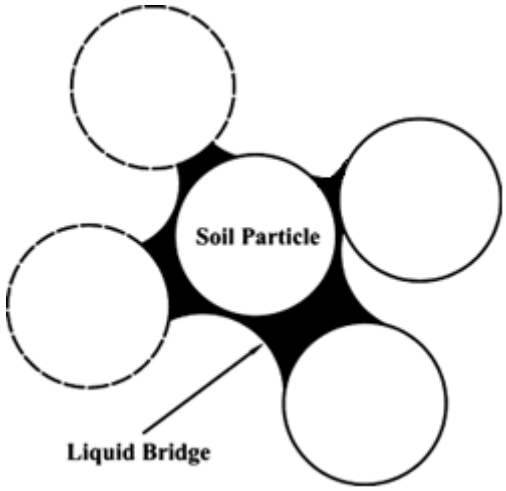

Figure 18: Coalescence of the liquid bridge. This happens to be a newly-constructed huge meniscus compounded by the water of four two-contact little bridges, existing before, whilst the filling angle was less than 30 degrees

We therefore tried to verify approximation [31] which was the case for a pair of particles, the results are further explained in Figure 28, as we can see, the less the amount of water, the more similar both parameters were (Sr and χ). From this we was able to conclude that with extremely small quantities of water, we could assimilate one to the other. Therefore, being within the pendular state, defined like the state of soil, where there is no coalescence between water bridges, meaning the filling angle was lower than 30°, normally established when its degree of saturation is between 0 to 5%.

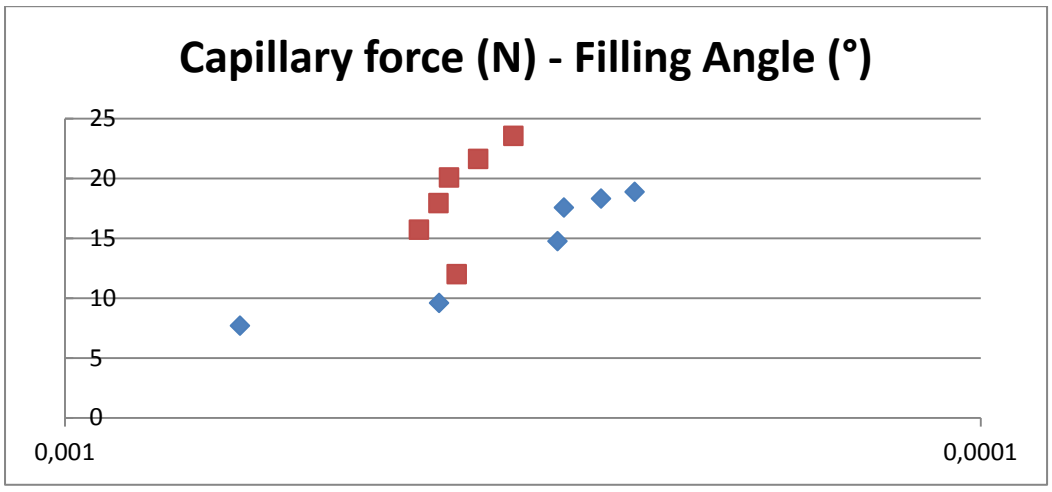

Figure 19: Clear decreasing in the intensity of the capillary force when the wetting angle is shown on a logarithmic scale

The filling angle is a sensitive parameter within the capillary force description, as is shown in Figure 19, with a marked relation between the capillary force and filling angle. To be able to appreciate the value of this parameter, photographs were taken throughout the course of the experiments on the measure of capillary forces. Picture 8 gives an example of a capillary doublet. It is verifiable in the photograph that the wetting angle is not null. In fact, the value of the wetting angle may vary considerably as a function of several factors sometimes making it difficult to evaluate: such as the impurity presence in the balls surface or in the water, the balls roughness… [32].

Additionally, the filling angle is not constant; it changes notably during the essay as can be seen in Figure 16. These results were obtained by treatment using the ImageJ program on a series of photographs taken during the course of the experiment.

Picture 8: Photograph of a capillary doublet

2.1.1.5. CALCULATIONS

For the micro-mechanical experiments, the total volume was calculated as the volume of a cylinder with the height of a ball's diameter and the same radius for a ball, which was 1 mm. We did this because we only considered the REV, i.e. the Representative Elementary Volume, which plays a central role in the mechanics and physics of random heterogeneous materials with a view to predicting their effective properties. A REV size can be associated with a given precision of the estimation of the overall property required and the number of accomplishments of a given volume V of microstructure that one is able to consider. Meaning that,

$$Vcilinder = \pi hr^2 = \pi Dr^2 = 2\pi r^3 = 6.28319E-09\, m^3 = V_{REV} \quad (11)$$

The volume of pores was obtained by taking away the volume of one ball, as in the REV we have one half of a ball, and half of another, which shows that:

$V_{total\ (RVE)}$	6,28319E-09	m^3
V_{ball}	4,18879E-09	m^3
V_{pores}	2,0944E-09	m^3

The porosity, n, was then obtained as a division between the volume of pores and the total volume of the sample, as we did further on within the macroscopic experiment.

V_{pores}	2,0944E-09	m^3
V_{total}	6,28319E-09	m^3
n	0,333333333	

We also obtained, another indicator of the soil state, the void ratio, e, and we acquired it by dividing the pores volume and the solid one.

V_{pores}	2,0944E-09	m^3
V_{solid}	4,20173E-09	m^3
e	0,498460018	

The last parameter of the soil that we obtained was the degree of saturation, Sr, calculated as a division between the water volume and the pores volume that we had within the Representative Elementary Volume. This is the initial and maximum degree of saturation within the experiment, because the evaporation will reduce progressively the parameter.

V_{water}	6E-10	m^3
V_{pores}	2,0944E-09	m^3
Sr	0,286478898	

2.1.2.SHEAR STRENGTH EXPERIMENTS

2.1.2.1. PUT IN CONTEXT

At the beginning of this thesis, we were supposed to obtain the shear strength on both a micro and micromechanical scale. However, the problem was that the technology we normally used was not appropriate, as we needed to recreate the shear essay for very small balls, which simulate the soil; this was something that became very difficult due to the tiny forces we had to apply and measure.

This meant that this year a test bed was designed by Maria Chiara Di Carlo [33], a student from Politecnico di Milano doing a double diploma exchange. Next year it will be constructed and

used by another student, from the Vrije Universiteit Brussel (the Flemish university of Brussels) Roos Evenepoel, who is going to further develop the issue of this paper in the next academic year.

To be able to accurately understand the interactions between balls within space, we considered an elementary volume, measuring the interaction between the balls that made up the following pyramid:

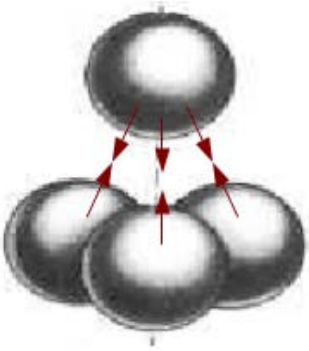

Figure 20: Interactions between grains to estimate from Ref. [33]

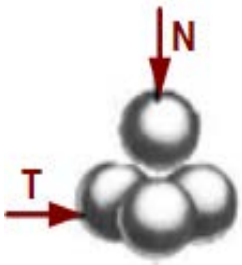

Figure 21: Forces applied to the system from Ref. [33]

2.1.2.2. THE GORGE METHOD

If we study the interaction between different balls, a normal force has to be applied. This force is the capillary force, already explained and defined following the "gorge method" (4), being:

$$N = 2\pi y_0 \gamma + \pi {y_0}^2 \Delta p \quad (4)$$

Where:

y_0 is half of the meniscus diameter when the spheres are in contact
γ is the surface tension
Δp is the difference in pressure.

Consequently, the test bed should have a system which allows constant normal force to be applied, N. The main objective was to see the minimal shear force that had to be applied, in order to cause the movement of the top ball in relation to the others. It is because of this, that the test bed had to provide a system allowing force T to be applied, and the means to be able to measure it.

Knowing that the playing forces, N and T, were very small (the order of magnitude is mN), the system had to be conceived with µN precision. By doing this, the error percentage of our measures should have been about 1%. Meaning the test bed was therefore designed as shown in Figure 22, with two independent systems, each one having one degree of freedom in translation.

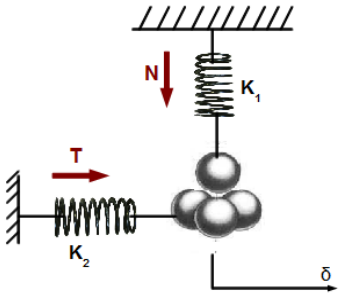

Figure 22: General system model. As we can see, in this test bed, there are two different systems, which have different stiffness and geometric properties [33]

We were interested in examining the situation when the balls were in contact; in this case, the top ball was fitted between the other 3 balls. The system should have therefore allowed the moving spheres aside and turned the three balls in order to see how each system configuration (one ball that is topped by one ball or one ball is between the other two balls) influenced the interaction between the balls. All this was done by keeping the normal force as steady as possible. In any case, the test bed had to be able to move the balls aside and to turn them. The ball translation had to cause a maximal variation of the normal force in order of 1%.

2.1.2.3. TEST BED REQUIREMENTS

In conclusion, the test bed had to:

- Apply a constant normal force, N, which depends on the capillary force and so to the radius R of the balls. Actually, the applied normal force is added to the capillary force; therefore at the end, the contact force is the sum of the normal applied force and the capillary force
- Perform a transversal displacement, δ_x
- Measure the force causing the transversal displacement, δ_x (shear force)
- Measure T with a maximal error on the order of 1%
- The conception should be done judicially, aiming to minimise the bulk and accomplishment costs
- Prepare for possibilities of adjusting and control to ensure that the balls are well placed, one in relation to the other.

The applied normal force must be of the same order of magnitude than the capillary force fixing the top of its value in $N = 5*F_{cap}$.

The capillary force between two spheres is defined by the Israelachvili in Ref. [34], as later explained in this paper. This formula has a proportional factor “cosθ”, the contact angle being θ.

Meaning, the capillary force depends on θ, and following our tests, our range of values on the contact angle is between 39 and 65, so the uttermost value is:

F_{cap} (θ = 39°) = 710.11 µN

N = 5 F_{cap} = 3.55 mN

The test bed had to be able to apply a constant force of 3.55 mN. The system that applied this load had to have a really weak stiffness (on the order of 0.3 N/m), calculated by the division of the variation of the normal force and the upwards displacement of the top ball, necessary for having lateral displacement.

2.2. MACRO-SCALE EXPERIMENTS

2.2.1.SHEAR STRENGHT EXPERIMENTS

2.2.1.1. TEST BED

The Direct Shear Test is used for determination of the consolidated drained (or undrained) shear strength of soils. The test is performed by deforming a specimen at a controlled rate on or near a single shear plane. The direct shear test is a laboratory testing methods used to determine the shear strength parameters of soil.

The test can be carried out at different moisture contents; however, it is common to saturate the sample before running the test. To achieve reliable results, the test is often carried out on three or four samples of undisturbed soil. The soil sample is placed in a cubic shear box composed of an upper and lower box. The limit between the two parts of the box is approximately at the mid height of the sample.

The sample is subjected to a controlled normal stress and the upper part of the sample is pulled laterally at a controlled strain rate or until the sample fails. The applied lateral load and the induced strain are recorded at given internals. These measurements are then used to plot the stress-strain curve of the sample during the loading for the given normal stress.

2.2.1.1.1. WATER DISPENSING

For the shear strength experiments we used a sprinkler. The reason for this choice is that we needed a homogeneous distribution of the amount of water, because we wanted to create the most numerous amounts of meniscuses possible, to be as close to the reality as possible. We then calculated the average water mass that the spray bottle expels with one compression. This is possible to see using the results placed in ANNEX 1.

The results are briefly shown below:

m(g)	recount	m(g)-mean(g)
0,65	1	-0,055915493
0,66	7	-0,045915493
0,67	5	-0,035915493
0,68	7	-0,025915493
0,69	11	-0,015915493
0,7	8	-0,005915493
0,71	4	0,004084507
0,72	7	0,014084507
0,73	4	0,024084507
0,74	2	0,034084507
0,75	2	0,044084507
0,76	1	0,054084507
0,77	1	0,064084507
0,78	2	0,074084507
0,8	2	0,094084507
0,82	1	0,114084507
0,83	1	0,124084507
0,84	1	0,134084507
0,85	1	0,144084507
0,87	2	0,164084507

Table 7: Water quantities from different squeezes

We obtained different statistics parameters, to certify that we were able to use the sprinkler, in other words, if the variability on the amount of water from each compression was or was not acceptable.

MEDIAN	0,7
MEAN	0,705915493
MODE (times)	0,69 (11)
STANDARD DESVIATION	0,002799983

As we can see, the values are very stable, meaning that we are able to trust in the linearity of the spray bottle. We can observe in the Figure 23 that the values are around average, with a shape ascribable to Normal distribution, tending to be to the right.

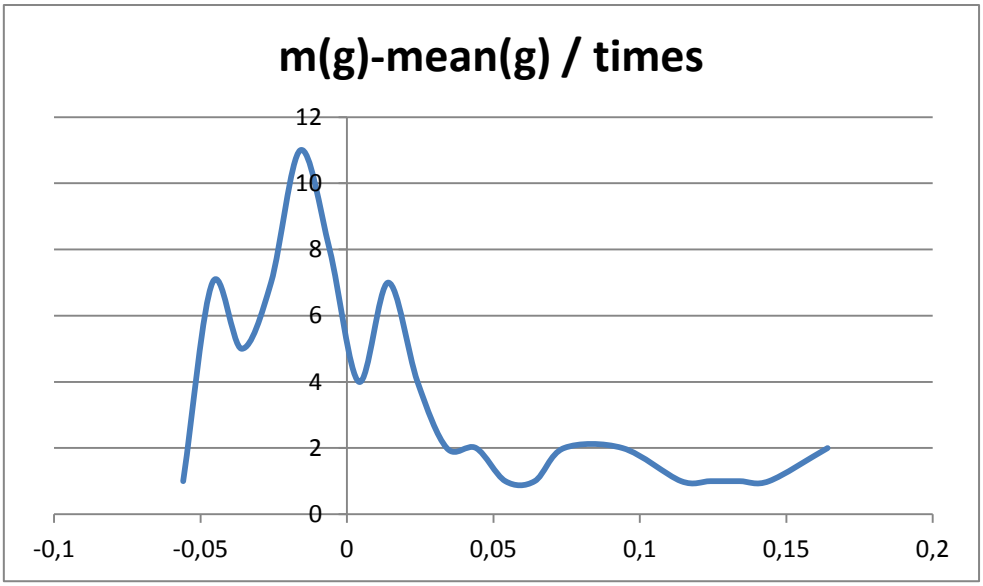

Figure 23: Distribution of the water content from each compression of the sprinkler, assimilable to Normal distribution (x-axis = amount of water with regard to the mean, y-axis = number of occurrence)

By doing that, we finally obtained the water mass that we assumed was to be rejected every time we pressed the sprinkler, and we got the volume by dividing by the well-known water density (1,000,000 g/m^3).

m_{spray}	0,705915493	g
V_{spray}	7,05915E-07	m^3

We then calculated the degree of saturation there would have been with one or several compressions on the spray bottle, dividing the water volume by the pores volume of the sample, as already calculated above.

spray (times)	V_{water} (m^3)	Sr
1	7,05915E-07	0,206556
2	1,41183E-06	0,413111
3	2,11775E-06	0,619667
4	2,82366E-06	0,826222

Table 8: Values of water volumes and the degree of saturation with every squeeze

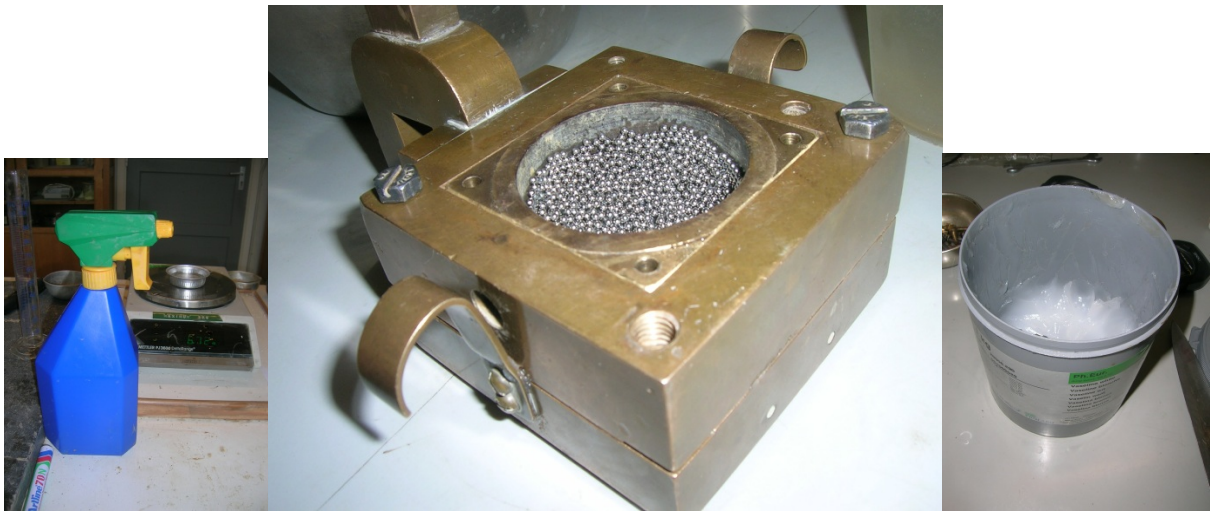

(a) (b) (c)

(d) (e)

Picture 9: Images of the material used during the shear strength tests: (a) Sprinkler, (b) Sample, (c) Vaseline, (d) Oven, (e) Weights

2.2.1.2. MODUS OPERANDI

1) Weigh the initial mass of the moisture in the pan.
2) Measure the diameter and height of the shear box.
3) Carefully assemble the shear box and place it in the direct shear device.
4) Then place a porous stone and a filter paper in the shear box.
5) Place the moisture into the shear box and level off the top.
6) Place a filter paper, a porous stone, and a top plate on top of the moisture
7) Remove the large alignment screws from the shear box
8) Open the gap between the shear box halves to approximately 0.1 cm using the gap screws, and then back out the gap screws.
9) Complete the assembly of the direct shear device and initialize the three gauges (Horizontal displacement gage, vertical displacement gage and shear load gage) to zero.
10) Set the vertical load (or pressure) to a predetermined value, and then close bleeder valve and apply the load to the soil specimen by raising the toggle switch.

11) Start the motor with selected speed so that the rate of shearing is at a selected constant rate, and take the horizontal displacement gauge, vertical displacement gage and shear load gage readings.
12) Record the readings on the data sheet. (You can also record the vertical displacement gage readings, if needed).
13) Continue taking readings until the horizontal shear load peaks and then falls, or the horizontal displacement reaches 15% of the diameter.

2.2.1.3. CALCULATIONS

The number of balls was calculated by dividing the total mass by the unitary mass of one ball; it was calculated by counting 30 and 27 balls respectively and measuring their weight, and then by dividing the results.

n(ball)	m(g)	m/n(g/ball)
30	0,99	0,033
27	0,89	0,032962963
4327,276811	142,72	0,032981481
4327	142,72	0,032983591

Table 9: Estimation of the number of balls

We then concluded that the number of balls was 4,327. Therefore the ball's volume was calculated as product of the ball unitary mass and the well-known steel density as (7,850,000 g/m^3), as follows:

n(ball)	m(g)	v(m^3)
1	0,032984	4,20E-09
4327	142,72	1,82E-05

Table 10: Mass and volume used in all calculations

We then obtained the total volume of the sample as follows:

$$V = \pi r^2 h \quad (11)$$

Where:

r is the radius of the sample

h is the height of the sample

Briefly,

V_{total}(m^3)	r(m)	h(m)
2,15984E-05	0,025	0,011

Table 11: Physical characteristics of the moisture

We calculated the volume of the pores simply by subtracting the balls' volume from the total volume of the sample. An example is found below.

V_{total}	2,15984E-05	m^3
V_{solid}	1,81809E-05	m^3
V_{pores}	3,41756E-06	m^3

We then obtained the porosity, n: as the division between the pores volume and the total volume of the sample.

V_{pores}	3,41756E-06	m^3
V_{total}	2,15984E-05	m^3
n	0,158231626	

We also obtained another indicator of the soil state, the pores rate, e, by the division of the pores volume and the solid one.

V_{pores}	3,41756E-06	m^3
V_{solid}	1,81809E-05	m^3
e	0,187975256	

2.2.1.4. NON-VALID RESULTS

Unfortunately, the final results of the shear strength experiments were not considered, due to the high disparity of the output values. The fact that the force captor was 50 g (maximum force of 200kg), which was not recognised as adequate for the scale of the normal force we applied, consisting of 332.22g, it was maybe a determinant for the non-validity of these results, as shown in Figures 24, 25 and 26.

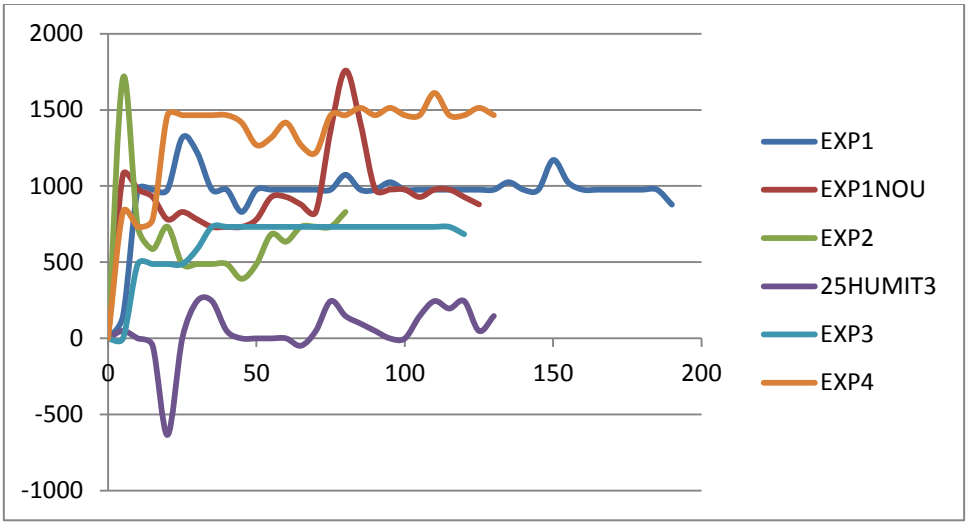

Figure 24: Results of several experiences with different contents of water, showing no agreement at all with the currently accepted geotechnical premises

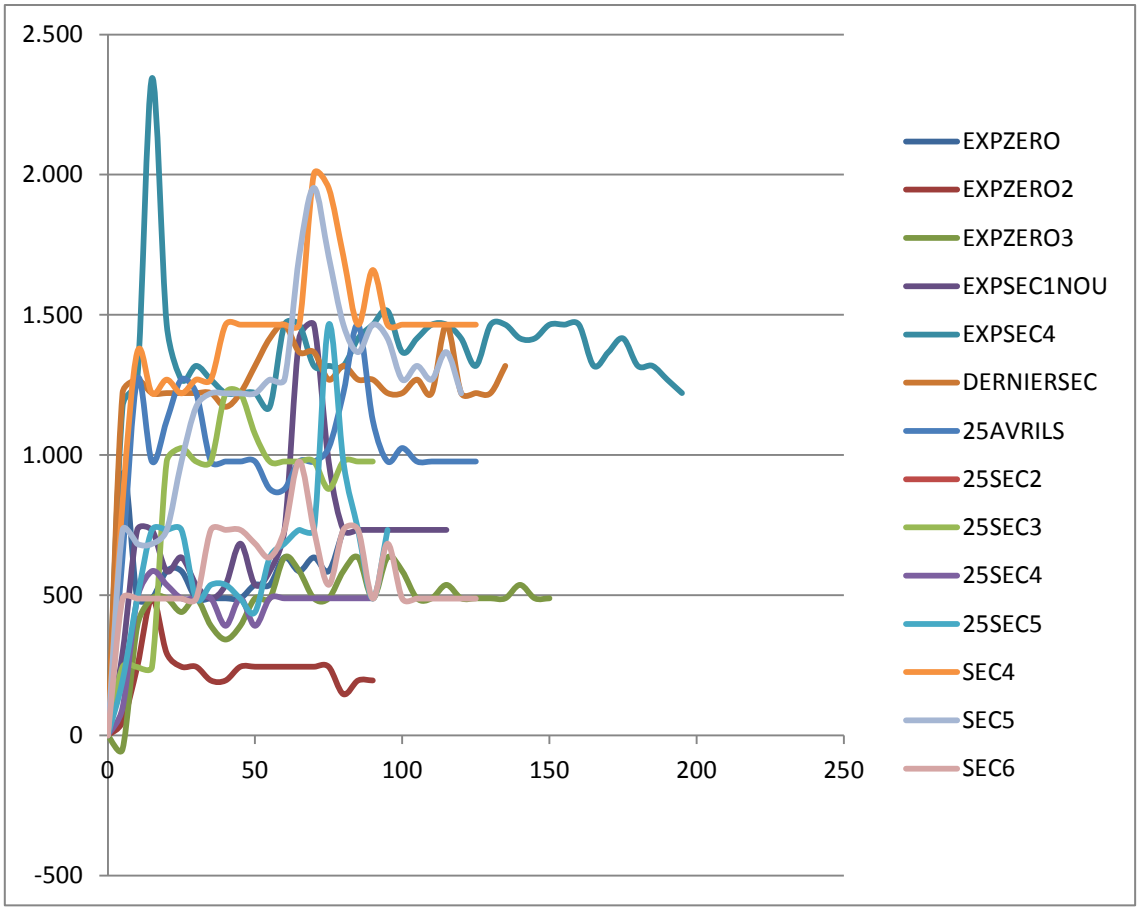

Figure 25: Different results, expressed by terms of kgf along the time (s), for the shear strength using the same quantity of water, being 0, the same normal force, the same particles (steel balls of 2mm diameter), the same captor of force, even the same laboratory assistant, demonstrate the lack of coherence in the system

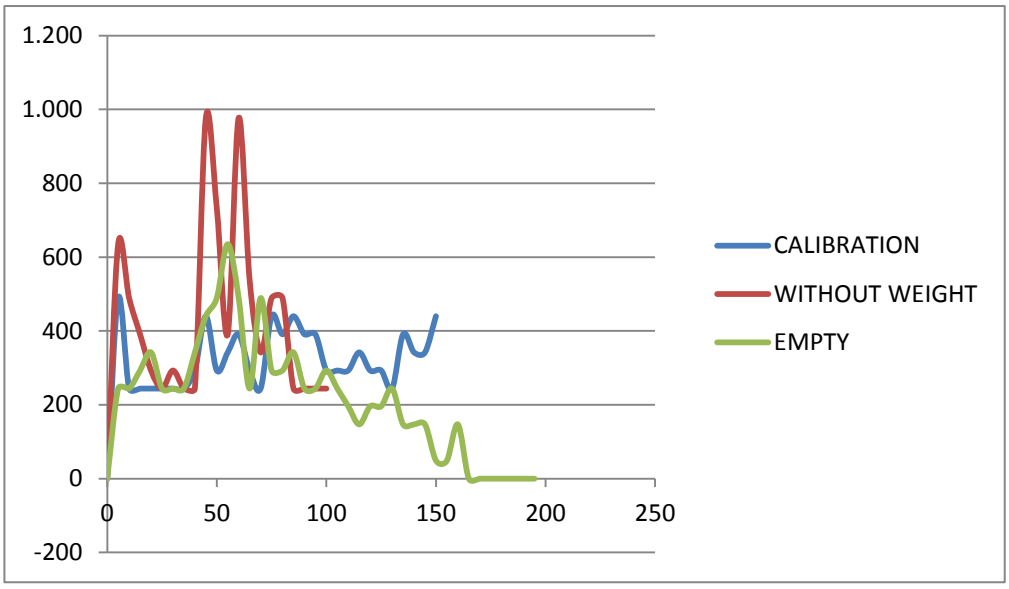

Figure 26: Results of the calibration of the system (carried out to be sure that is in order), and the moisture without normal force applied and without anything inside

After an accurate analysis, we concluded that probably the results were strongly affected by the friction between the two half-box of the device. As we can see in Picture 9 with other material, it was used Vaseline what for sure severely limits the friction between the two half-boxes, but there are probably other sources of friction that cannot be avoided. A dry empty test (without balls) was carried out showing certain resistance as depicted in Figure 26. This probably comes from the friction resistance of the entire device.

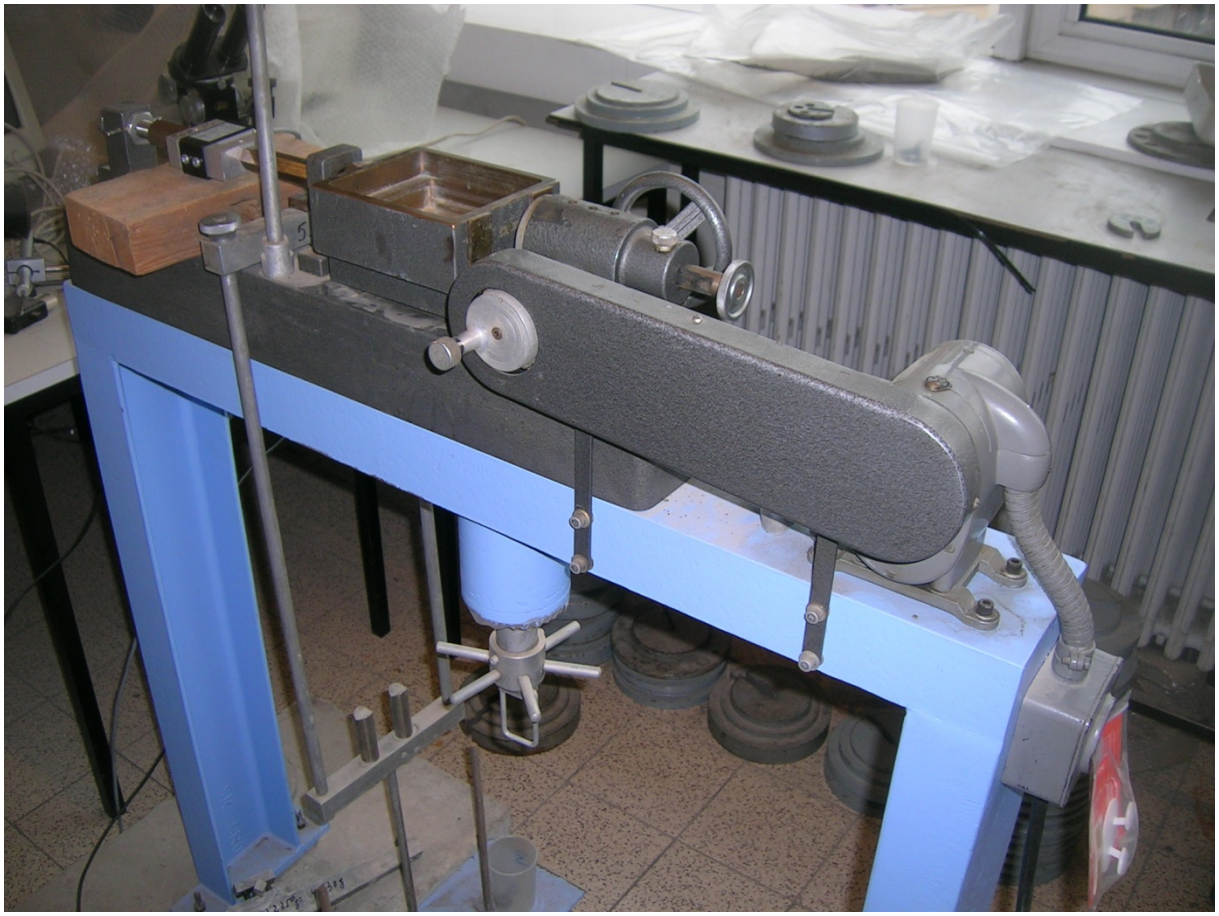

Picture 10: Shear strength test bed, part of the geotechnical laboratory of ArGEnCo (Architecture, Géologie, Environnement et Constructions), ULB

3. THEORETICAL STUDY

3.1.ISRAELACHVILI FORCE

Let us consider a sphere with the radius R, located at a distance z from a surface. The liquid meniscus rises up to a height D+2h (the immersion height h is so that the filling angle θ is small). By considering a constant volume of liquid, Israelachvili [33] calculated that the attractive force between the sphere and the surface due to the liquid is:

$$F_{cap} = \frac{4\pi\gamma R cos\theta}{1+\frac{D}{h}} \quad (12)$$

Where:

γ is the surface tension of the liquid

θ is the contact angle

D is the gap between the sphere and the surface

R is the radius of the ball

h is the height of the wetted perimeter

This formula (12) does not depend on the liquid volume whilst there is contact.

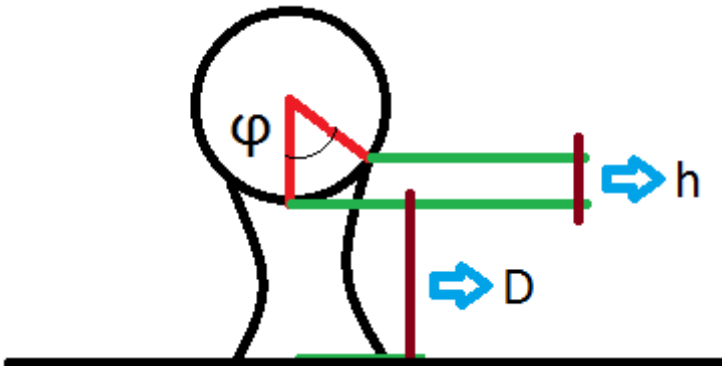

Figure 27: Conclusion of the used distances in the Israelachvili formula [33]

In the case of the contact between two spheres, this force is calculated as:

$$F_{cap} = \frac{2\pi\gamma R cos\theta}{1+\frac{D}{2h}} \quad (13)$$

Where:

D is the gap between both spheres

h is the height of the wetted perimeter

γ is the surface tension of the liquid

θ is the contact angle

R is the radius of the balls, in case of monodispersity, as in our paper. In case of polydisperse material R is defined as the harmonic mean of the different radius, i.e.

$$\frac{1}{R} = \frac{1}{R_1} + \frac{1}{R_2} \quad (14)$$

As the distance between the spheres is zero in this work, this force is expressed as:

$$F_{cap} = 2\pi\gamma R cos\theta \quad (15)$$

Being, this formula, just the vertical component of the traction force created by the water's presence.

Finally, we obtained the effective stress by dividing the capillary force by the section of the ball.

3.2.χ, THE EFFECTIVE STRESS PARAMETER

As seen in the state of the art of this work, in determining the behaviour and strength of unsaturated soils, it becomes difficult to choose the controlling stress variable that would substitute for the role of effective stress in the saturated case. Bishop (1959) extended Terzaghi's effective stress principle to account for the presence of an air phase by intuitively introducing an average pore fluid pressure weighted over the pore air (u_a) and water (u_w) pressures, i.e.

$$\sigma' = \sigma - [\chi u_w + (1-\chi)u_a] = (\sigma - u_a) + \chi(u_a - u_w) \quad (16)$$

Where σ and σ' are the total of effective stresses respectively, and χ is the weighted parameter that is arbitrarily confounded with the degree of saturation, Sr, calculated above.

The effective stress parameter χ emerges as the isotropic part of the integral, giving the distribution of liquid bridges. For each meniscus connecting a pair of particles, we readily compute the fabric tensor as [30],

$$F_{ij} = \int_{\Gamma_w^p} n_j n_i d\Gamma = \frac{\pi R^2}{3}\begin{bmatrix}\lambda_1 & 0 & 0\\ 0 & \lambda_2 & 0\\ 0 & 0 & \lambda_3\end{bmatrix};\ \lambda_1 = 2(1-cos^3\alpha) \text{ and } \lambda_2 = (1-cos\alpha)^2(2+cos\alpha) \quad (17)$$

Where:

α is the filling angle, obtained by the photograph taken whilst the micro-scale experiments

Γ_w^p is the integration domain, being the wetted surface by the meniscus

According to equation (17), F_{ij} is a symmetric tensor with its first invariant, δ_{ij}*trace*(**F**), being independent from the rotation in the coordinate system. The explicit expression of the effective stress parameter for different packing's of spherical particles can thus be derived, i.e.

$$\chi = \phi S_r + \frac{2\pi R^3}{9V} L(\lambda_1 + 2\lambda_2) = \phi S_r + (1-\phi)\frac{L}{6N}(\lambda_1 + 2\lambda_2) \quad (18)$$

Where:

ϕ is the porosity, usually noted as n

S_r is the degree of saturation

R is the radius of the ball

V is the stocked water volume

L is the number of liquid bridges

N is the number of balls

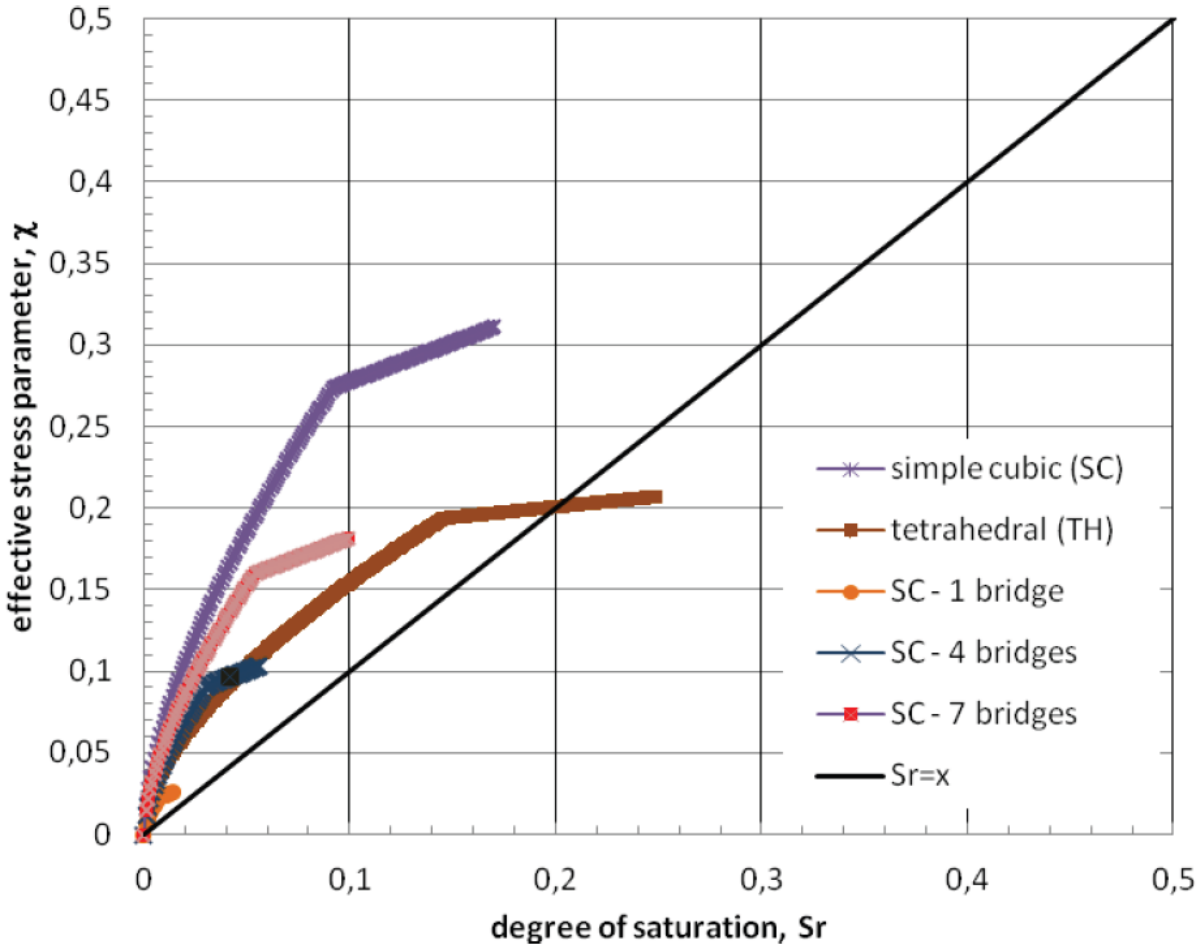

Figure 28: Computed relationship between degree of saturation Sr and the effective stress parameter χ from Ref. [30]

The simulations revealed that both packing and the number of liquid bridges influenced the shape of the χ vs. Sr curve. For instance, the tetrahedral packing gave much lower χ values than those associated with the simple cubic packing for the same degree of saturation. As one would also expect for the same packing with a decreasing number of liquid bridges, lower values of χ were predicted for the same degree of saturation because of a decrease in overall suction. It should be noted that the range of degree of saturation, examined in the numerical computations based on idealised mono-sized spheres, was well below 30% since the menisci were not allowed to merge to give full saturation. The restriction of packing to rather simple configurations with mono-sized spherical particles could plausibly account for the difference between experimental and computed data. This matter will require a more detailed investigation. At any rate, it is also not evident if the experimental data in the range of small degree of saturation investigation (less than 30%) is accurate and reliable, given the known difficulties in measuring low suction in soils.

As we can observe, the result obtained for the searched parameter was the half of the degree of saturation, which at first was considered to be a mistake, but partly corroborated by Figure 28, extracted from Ref. [31], the same paper where we found the numerical approximation that we implemented, this shows the computed effective stress values as a function of degree of saturation with the line χ = Sr also plotted here as a reference. All simulations produced a curve that plots above the χ = Sr line showing a perceptible bend with a break in slope at some characteristic degree of saturation when the water meniscus reached its maximum filling angle α_{max}. Subsequent filling then proceeded at fixed wetting points on the particle whilst the curvature of the meniscus continued to decrease towards reaching a larger water volume.

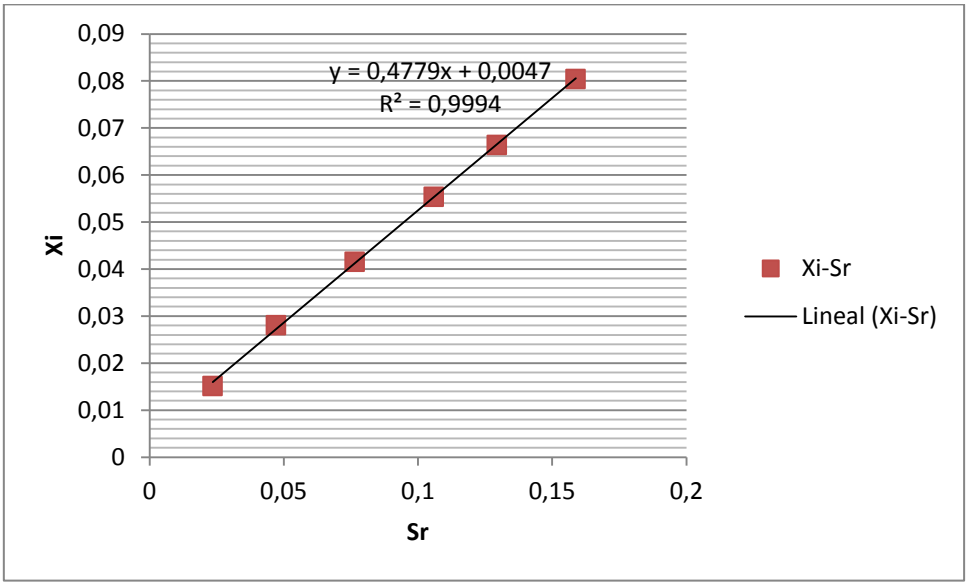

Figure 29: Comparison of the obtained parameter's, Sr and χ_i, for different water contents

We then obtained the effective tension, by our first approximation:

$$\sigma' = s\chi_i \quad (19)$$

s being the suction and χ_i the effective stress parameter, comments found below.

We obtained this suction by measuring the internal diameter of the meniscus and the radius of the circles, which were tangents to both sides of the meniscus.

The water volume, initially of 0.6µl, was deduced supposing linear evaporation celerity. The suction was deduced from:

$$S = \gamma(\frac{1}{r_1} + \frac{1}{r_2}) \quad (20)$$

Where:
γ is the surface tension
r_1 is the radius intern of the meniscus
r_2 is the average of the two radius (left and right) tangent to the meniscus.

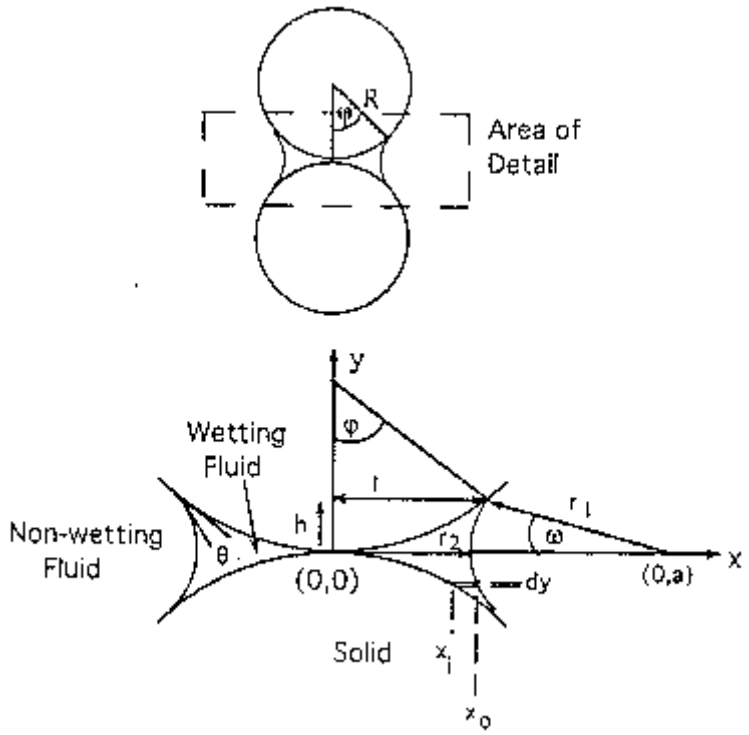

Figure 30: Cross section of a pendular ring of wetting fluid surrounding the point of contact of two identical spherical particles, with parameters defined from Ref. [35]

4. NUMERICAL SIMULATION:

4.1. PRINCIPLES AND ASSUMPTIONS

This work provides an estimate of the effective stress in unsaturated soil using different percentages of water, both theoretically and experimentally. The two estimates were compared, to contrast the validity of the numerical simulation; by a Matlab routine, which calculates the meniscus shape between two spheres, the water pressure and the capillary force. Actually, this code is not an approximation, but it is the exact solution of the differential equation:

$$Total\ curvature = \frac{Pressure\ difference}{Surface\ tension} \quad (21)$$

The meniscus research was doubly iterative; a priori we did not know the position of the triple line nor the pressure within the water bridge. If this double loop did not converge, what happened for example in the case that we impose more water than the meniscus could absorb (i.e. χ = 0.5 with θ = 10°), the iteration stopped, but the post-treatment, which included the force calculation, was made for the last running meniscus. This result therefore did not have to be taken into account; it had no validity, and did not make sense, as it did not correspond to the meniscus that we expected.

Our numerical simulation, well-understandable using Figure 31, also gives a diagram of the meniscus shape (Figure 32) and a chart showing the evolution of the effective stress obtained using Bishop's correction for the different given effective stress parameter, χ (Figure 33).

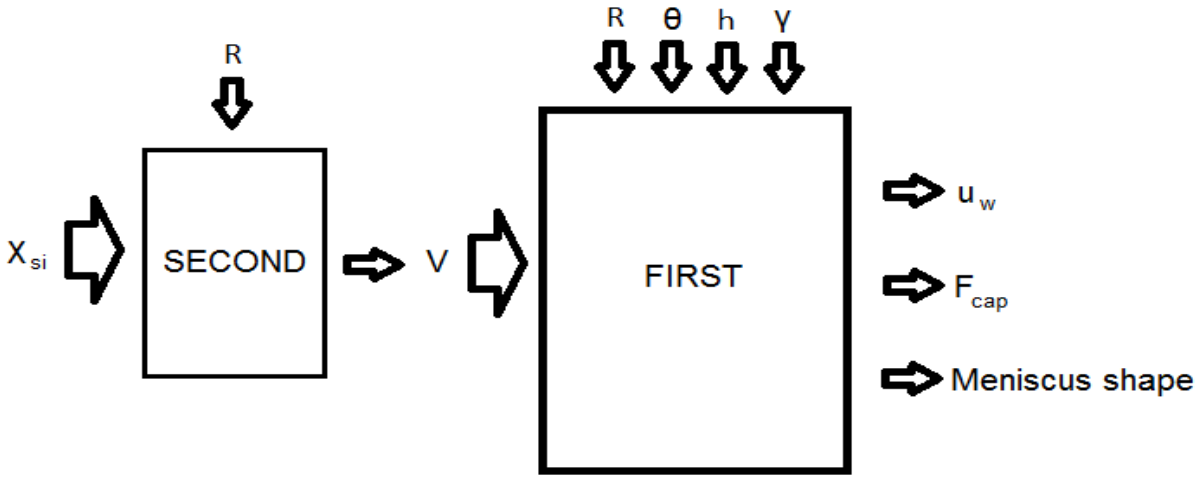

Figure 31: Overview of the input and the output of the implemented model

The main assumptions of the model were as follows:

- Gravity was neglected toward the capillary force.
- Contact angle hysteresis was not taken into consideration.
- Dynamic contact angle was not taken into account.
- Materials were assumed to be smooth (no roughness) and without any impurities.

- Inertial forces acting on the liquid bridges were neglected, which was not valid if the release task was based on acceleration of the gripper.

4.2. FUNCTION FIRST

The routine *FIRST*, contained in the ANNEX 2, calculated the meniscus shape in-between two spheres, the water pressure, and the capillary force. The incoming data was:

- R: the spheres radius (0.001 meters),
- theta: the contact angle θ (50.598 degrees introduced in radians),
- h: the distance between the two balls, which was supposed as zero throughout this project,
- gamma: the surface tension γ (0.072 N/m).
- V: the liquid volume, which was calculated by the product of two values coming from another function, called SECOND, which runs the code *FIRST* for different given volumes, calculated as a function of:
    - Xsi: the effective stress parameter χ, previously defined, and was evaluated for different values ranging from 0.0001 to 0.01 (`Xsi=linspace(0.0001,0.01,20)`).
    - interstitial_volume: calculated, as we have seen previously, like the Representative Elementary Volume (estimated as the volume of a cylinder with the height of the diameter of the balls, and the base as the radius) minus the volume of one ball, which was the volume of one ball, as the cylinder considered is contains half of the lower ball and half of the upper one (2.0944E-09m^3).

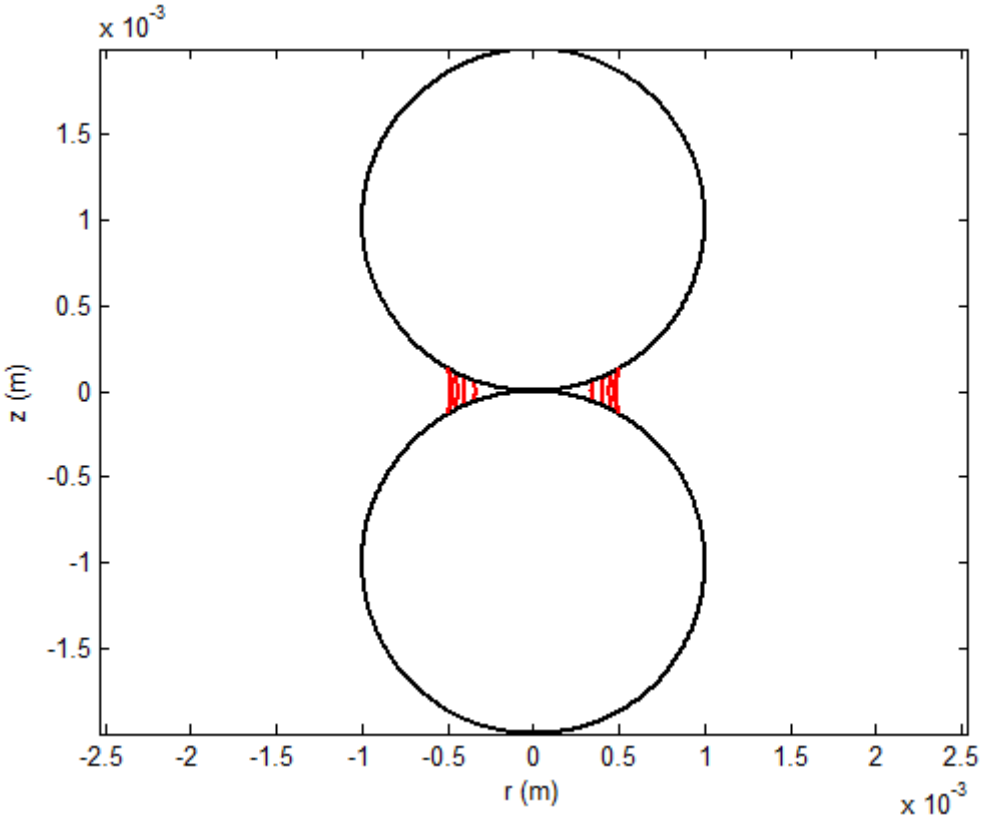

Figure 32: Image given by the routine, showing the different meniscus for the different amounts of water

4.3. FUNCTION SECOND

The function *SECOND*, contained in the ANNEX 2, calculated the water pressure by multiplying the liquid bridge curvature by the surface tension and adding up the air pressure, considered as 101,325 Pa. It then also produced the Bishop's approximation (5) viewed on the state of the art of this paper.

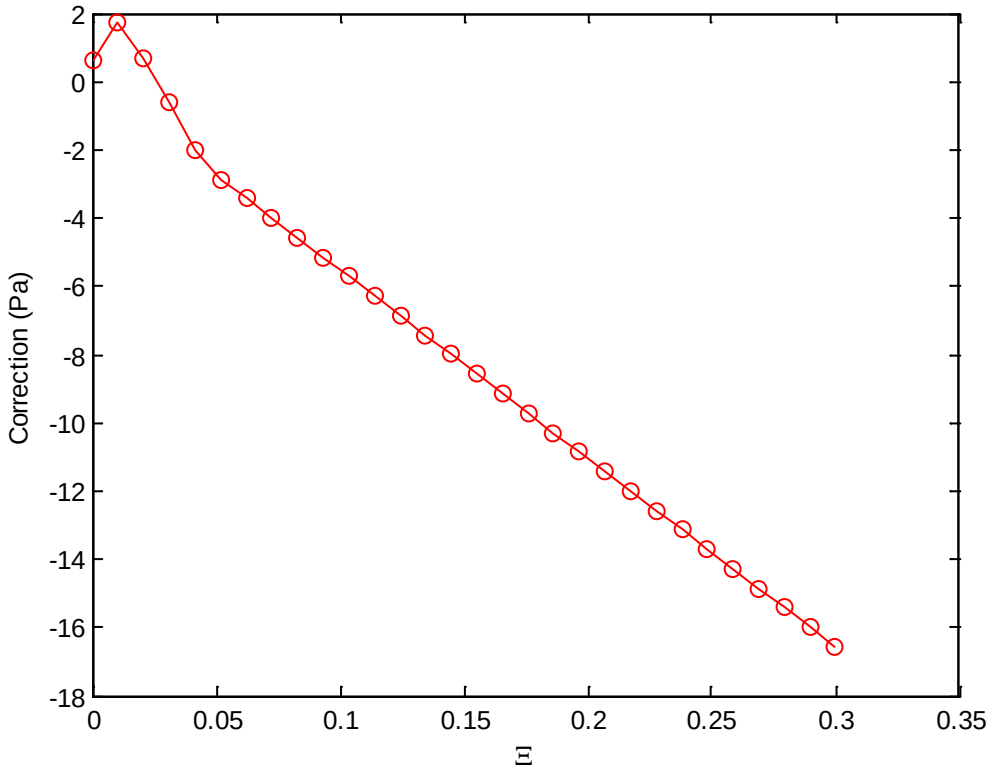

Figure 33: Image given by the routine, showing the evolution of the effective stress obtained using Bishop's correction for the different given effective stress parameter, χ

RESULTS COMPARISON

I therefore compared the capillary force due to the presence of water depending on:

- Whether we obtained it using the Israelachvili force approximation, i.e. the vertical component of the traction force created by the water's presence,
- If it was produced by the establishment of a microscopic model of the liquid bridge, properly explained in the numerical simulation chapter or,
- If we obtained it by measuring the deflection of the beam and multiplying it by its stiffness or
- Whether it was produced by multiplying the suction by the effective stress parameter and multiplying by the section of one ball. The criterion for obtaining these parameters has been explained in the theoretical study.

As we were within a state of absence of the exterior force (which tended to put the spheres in contact but not by means of capillary) the theoretical effective stress was equal to Bishop's correction, with the force, given by Matlab, divided by the overall section (for the case of two spheres, it is πr^2).

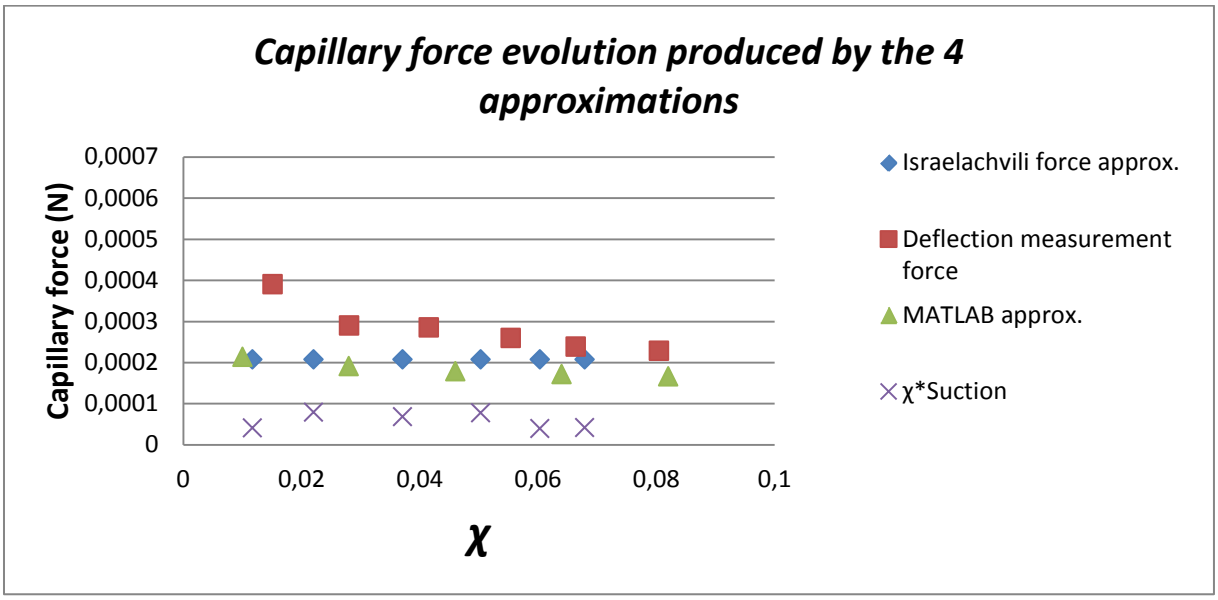

Figure 34: Different obtained values with the four different approximations, as previously explained

The conditions for which these approximations have been the follows:

Theoretical force approximation:

1. θ, the contact angle*
2. γ, the surface tension of the liquid
3. D, the gap between the two balls, in our paper, always supposed as 0, due to the grains of soil they are mostly in a contact situation, usually noted as h
4. R, the radius of the ball

Deflection measurement force:

1. δ, the deflection measurement
2. k, the stiffness of the plastic beam, calculated by measuring the deflection of the beam with three weight-known small objects, placed around the glued ball.

MATLAB approximation (containing the Israelachvili formula):

1. R, the spheres radius
2. θ, the contact angle*
3. h, the gap between the two balls, in our paper, always supposed as 0, due to the grains of soil they are mostly in a contact situationγ, the surface tension of the liquid
4. V, the liquid volume, which was calculated as a function of χ and the interstitial volume

χ x Suction approximation:

1. γ, the surface tension
2. r_1, the intern radius of the meniscus*
3. r_2 , the average of the two radius (left and right) tangent to the meniscus*
4. ϕ, the porosity, usually noted as n
5. S_r, the degree of saturation
6. R, the radius of the ball
7. V, the stocked water volume
8. L, the number of liquid bridges
9. N, the number of balls
10. α, the filling angle*

The values obtained agree with the others, as we can clearly see in Figure 34, we can then conclude that the four approximations are appropriate for the conditions given. We can notice the force diminution with the increasing of the liquid volume, what was the expected tendency. Nevertheless, it is noticeable that the "χ x Suction" approximation produced results clearly lower than the real force. This could be explained by the Figure 26, where we can see that for weak quantities of water (lowers than χ = 0, 1) real curve is above the diagonal χ = Sr.

* obtained by the photograph taken whilst the micro-scale experiments

SUMMING-UP

STATEMENT

The objective of this study was twofold. On the one hand, it was to study the interactions of capillary force between particles of a granular medium, and on the other it was to study the effect of these interactions on macroscopic behaviour. The balance sheet below highlights three important aspects of this thesis. The first aspect is about the need for more precise approximations to come to a more realistic distribution of effective stress in unsaturated soils, the second is devoted to the study of cohesion by capillarity in the presence of a solution of pure water. And the last aspect, gives four lines which give a brief summary of this work.

Starting with the classical definition of the effective stress in saturated soils and looking at the evolution of the previous century, where unsaturated soils had been the object of studies; we discussed existing expressions of the effective stress in unsaturated soils used in engineering calculations. Based on the two stress variable formulation accepted for unsaturated soils, some definitions of generalised effective stress were proved. It simultaneously suits the numerical simulation and a set of experiments in granular media, trying to get a contribution from the micro to the macro-scale, always working with unsaturated soils.

A literary review shows that capillarity is a major mechanism of cohesion, something that is important to take into account when one is interested in wet granular media. It also shows how complex this phenomenon is, given the multiplicity of the parameters that condition it. A good opportunity to study the sensitivity of capillary force of these various parameters through micro and macro approaches. These approaches require a good characterisation of local interactions and their integration into macroscopic modelling. Such an approach is twofold. The first has been adapted to the geometric conditions of the study, such as the triple line research. The second component consists of building a computer code relating to the proposal of an effective stress law taking into account the capillary phenomena at a micro scale, as we have within unsaturated soils.

The points put forward by the characterisation of a capillary force law follow on from the desire of leaving the physical phenomena at a local level. This physics should integrate the polydisperse character of the soil reflecting the granularity often spread by granular media. In addition, the physics should take into account the characteristics of the components and their possible thermodynamic evolutions. These considerations, force the choice of an explicit expression from the capillary cohesion law. The proposed law expresses the capillary force depending on the geometric configuration of the grains, the intergranular distance (supposed as 0 in this work), the volume of the liquid bridge and the characteristics of components such as the surface tension of the liquid, the wetting angle ... This law has been elaborated on the basis of a coupled theoretical and experimental approximation on the local scale, the originality of which lies in its explicit nature which needs a minimal amount of calculations before taking into account the various parameters where the capillarity is included.

Simulations and experiments were performed under the same conditions of geometry, water contents scale, and similar conditions of granularity. The curves (figure 34) present the results that were obtained both numerically and experimentally were quite similar, not in terms of evolution but in order of magnitude. This shows the ability of computer code to satisfactorily describe the influence of capillary cohesion on the behaviour of a wet granular material.

OUTLOOK

At the end of this study, direct extensions to this work seem natural to bring a better understanding of the effects of the presence of liquid on the mechanical behaviour of granular media. These extensions are presented here in two categories. The first refers to the shear strength increase on the capillarity, which we tried to obtain at a macro-scale, but with invalid results due to the lack of precision in the dispositive. Other kind of micro-scale experiments should also be done, in the near future and a bed test allowing the measurement of capillary forces in shear strength should have been designed [33] and next year it will be constructed and used by another student, who will further develop the issue of this paper during the next academic year.

The second extension deals with an opening to thermodynamic studies of the mechanical behaviour of wet granular media; such as the effect of temperature and the presence of a solute in water. Indeed, one of the peculiarities of the phenomenon of cohesion by capillarity lays in its essential coexistence with the phenomena of transfers. By their nature; capillary phenomena are associated with the presence of liquid water in the granular medium. Unlike the solid skeleton, this water is a component particularly sensitive to interactions with the environment. It may be the seat transfer, phase changes and act as a vector of solutes. These phenomena are themselves temperature dependent. In this context, for future investigations and without going into a full thermodynamic study of the liquid bridge, it would be interesting to emphasise on the first approach of the effect of temperature and the presence of a solute which can be optionally crystallised.

In this study, a series of difficulties were made apparent and tried to circumvent on the first approach. These difficulties were related to a misunderstanding on the evolution of the contact angle, and their hysteresis phenomena and the effects of the viscosity of the liquid on the sliding contacts and cohesion. Indeed, this angle presents an evolution complex and a strong dependence on environmental conditions. It significantly influences the intensity of the capillary force so as to warrant an in-depth study. With regard to the phenomena of hysteresis, a detailed analysis of these effects at a macroscopic scale should be considered, especially for the cyclic loading case. Moreover, the distribution of liquid within granular materials is a key point in the study of wet granular materials. A thorough experimental study of the distribution and size of liquid bridges within granular materials is necessary to verify the validity of the criterion of the used distribution and if appropriate, to propose another one.

It has not been part of the work, due to lack of time, but it would have been interesting to have been able to generalise this contact between two spheres with a contact network of a different assembly of spheres; i.e. a cubical network (4 spheres forming a cube), a tetrahedral network (3 spheres forming a pyramid)… allowing more realistic results to be achieved. For any case, the following should be deduced:

- The maximum volume (linked to the effective stress parameter χ) admissible before having coalescence of the meniscus between spheres (for a realistic wetting angle),
- The vertical effective stress expression (the projection of the correction in the vertical direction). This second point, within the cube case, does not have to be deduced, as the effect is already strictly vertical.

Indeed, the influence of water, within the mechanical behaviour of granular media, results from several phenomena exceeding the framework of capillary force. Thus, approaches into discrete elements may constitute relevant analytical tools in studying other phenomena associated with the presence of water. Our routine is simply an analytical resolution of the capillary tension between two spheres, but DEM (Discrete Element Method) proposed by Cundall [36] in 1971 is becoming widely accepted as an effective method of addressing engineering problems in granular and discontinuous materials, especially in granular flows, powder mechanics, and rock mechanics. A distinct element method is a powerful method providing the interaction forces between particles well characterised, in fact, that justifies the aim of this work, because the mechanical behaviour modelling within unsaturated granular media with DEM, requires knowing the capillary forces. This method is from any family of numerical methods for computing the motion of a large number of particles of micrometre-scale size and above. It is an interesting alternative to the FEM (Finite Element Method) that deserves to be widely developed for the fine results is already produces; with advances in computing power and numerical algorithms for nearest neighbour sorting, it has become possible to numerically simulate millions of particles on a single processor. Among these phenomena, cases of phase changes, related to variations in temperature and the presence of solutes in liquid bridges, is an interesting opening in the granular approaches to the thermodynamics and chemistry fields.

Furthermore, throughout this study, the solid grains have been insensitive in supposing the presence of water. Though, in many applications, the shrinkage or swelling of the grains during drying or imbibition may be of significant interest. Extensions of the approach presented in this study are therefore possible in this direction; it is possible to numerically model the deformation of grains by introducing the kinetics of shrinkage or swelling into the code from the experience on the computer.

To summarise; the geometric parameters, physical and thermodynamic properties involved in the description of phenomena associated with the presence of liquid in granular media obviously do not have the same degree of importance in a given situation, what it deserves to be widely studied, to be able to give the proper weight to each parameter whilst it calculation. This fact imposes a view of synthesis in order to prioritise the respective effects of these parameters and to identify their relevance according to context.

REFERENCES

[1] Pierre Lambert. *Capillary Forces in Microassembly; Modeling, Simulation, Experiments, and Case Study*. Microtechnology and MEMS. ISBN 978-0-387-71088-4.

[2] Fabien Soulié. *Cohésion par capillarité et comportement mécanique de milieux granulaires*. 2005.

[3] E. Alonso, A. Gens and A. Josa. *A constitutive model for partially saturated soils*. Géotechnique, 1990, vol. 40, no. 3, pp. 405-430.

[4] K. Hotta, K. Takeda, K. Iionya. *The capillary binding force of a liquid bridge*. Powder Technology 1974; 10:231-242.

[5] G. Lian, C. Thornton, M. J. Adams. *A theoretical study of the liquid bridge force between rigid spherical bodies*. Journal of Colloid and Interface Science 1993; 161:138-147.

[6] Mathieu Nuth and Lyesse Laloui. *Effective stress concept in unsaturated soils: Clarification and validation of a unified framework*. International Journal for Numerical and Analytical Methods in Geomechanics.

[7] Bishop, A. W. and G. E. Blight (1963). *Some aspects of effective stress in saturated and partly saturated soils*. Geotechnique, vol. 13, n°3, pp. 177-197.

[8] E. Alonso and A. Lloret. *Comportamiento de suelos parcialmente saturados*. Revista de Obras Públicas, Mayo-Junio 1985. 435 a 461.

[9] Matyas, E. L. and H. S. Radhakrishna (1968): *Volume change characteristics of partially saturated soils*. Geotechnique, vol. 18, n°4, pp. 432-448.

[10] Miguel Angel Alfaro Soto. *Geotecnia en suelos no saturados*. Rev. Acad. Colomb. 32 (125): 471-481, 2008. ISSN 0370-3908.

[11] Jim Frankenfield. *Volumes and areas of pendular rings with non-zero contact angles*. 877-604-0166.

[12] L. Prabakaran, M. Prushothaman and P. Sriganesan. *Pharmaceutical Micropellets: An Overview*.

[13] F. Gabrieli, S. Cola, P. Lambert and F. Calvetti. *Micromechanical modelling of erosion due to evaporation in a partially wet granular slope*. International Journal for Numerical and Analytical Methods in Geomechanics. Int. J. Numer. Anal. Meth. Geomech. (2011). wileyonlinelibrary.com. DOI: 10.1002/nag.1038.

[14] S. J. Jiménez Salas. *Hacia una mecánica de Suelos no Saturada*. Revista Ingeniería Civil v. 88 – 1ª parte, pág. 145-164.

[15] D. G. Fredlund and H. Rahardjo. *Soil mechanics for unsaturated soils*. New York. John Wiley & Sons, Inc 1993. P. 1-6.

[16] D. Croney and J. D. Coleman. *Pore pressure and suction in soil*. Conference on Pore Pressure and Suction in Soils. London. P. 31-37.

[17] D. G. Fredlund, A. Xing and S. Huang. *Predicting the permeability functions for unsaturated soil using the soil-water characteristic curve*. Canadian Geotechnical Journal, 31(4): P. 533-546.

[18] Aikaterini Tsiampousi supervised by L. Zdravkovic and D. M. Potts. *Numerical Analysis of Excavations in Unsaturated Soils*.

[19] D. M. Newitt, J.M. Conway-Jones. *A contribution to the theory and practice of granulation*. Transactions of the American Institute of Chemical Engineer 1958; 36: 422-442.

[20] L. Bocquet, E. Charlaix et F. Restagno. *Physics of humid granular media*. Compte Rendu de Physique de l'Académie des Sciences, 3: 207-215, 2002.

[21] Jean-Yves Delenne, Fabien Souilié, Moulay Saïd El Youssoufi, Farhang Radjai. *From liquid to solid bonding in cohesive granular media.* July 2011.

[22] L. Picarelli, L. Olivares, L. Comegna, E. Damiano. *Mechanical aspects of flow-like movements in granular and fine grained soils*. Rock Mechanics and Rock Engineering 2008; 41(1): 179-197.

[23] M. Hürlimann, A. Ledesma, J. Martí. *Characterisation of a volcanic residual soil and its impications for large landslide phenomena: application to Tenerife, Canary Islands.* Engineering Geology 2001; 59(1-2): 115-132.

[24] B. D. Collins, N. Sitar. *Geotechnical properties of cemented sands in steep slopes*. Journal of Geotechnical and Geoenvironmental Engineering 2009; 135(10): 1359-1366.

[25] A. L. Barabási, R. Albert, P. Schiffer. *The physics of sand castles: máximum angle of stability in wet and dry granular media*. Physica A: Statistical and Theoretical Physics 1999; 266(1-4): 366-371.

[26] S. Nowak, A. Samadani, A. Kudrolli. *Maximum angle of stability of a wet granular pile*. Nature Physics 2005; 1: 50-52.

[27] Georges Asch. *Les capteurs en instrumentation industrielle*. Dunod, 1999.

[28] H.A. Rothbart. *Mechanichal Design Handbook*. 1996, Mcgraw-Hill Professional Publishing, ISBN 0-07-054038-1.

[29] http://www.ramehart.com/newsletters/2008-02_news.htm

[30] B. Capella and G. Dietler. *Force-distance curves by atomic force microscopy*. Surf. Sci. Rep., 31:1-104, 1999.

[31] R. Wan, S. Khosravani and F. Nicot. *Micromechanical analysis of stress in an unsaturated granular medium*.

[32] Maria Chiara di Carlo, tutored by Pierre Lambert. *Conception d'un banc d'essai pour mesurer les interactions entre les grains d'un sol non saturé*.

[33] J. Israelachvili. *Intermolecular and surface forces*. Academic Press, Londres, second edition, 1992.

[34] P. G. De Gennes, F. Brochard-Wyart and D. Quéré. *Gouttes, bulles, perles et ondes*. 2002.

[35] Xun Li, Lirong Zhong and Laura J Pyrak-Nolte. *Physics of partially saturated porous media: Residual Saturation and Seismic-Wave Propagation*. Annual Review of Earth and Planetary Sciences, Vol. 29: 419-460. May 2001.

[36] P. A. Cundall and O. D. L. Strack. *A discrete numerical model for granular assemblies*. Geotechnique, 29:47-65, 1979.

AUXILIARY INDEX

LISTE DES FIGURES

LISTE DES TABLES

LISTE DES PICTURES

ANNEX 1

CALCULATIONS

The data used for obtaining the average amount of water considered was displayed by each compression of the sprinkler:

m(g) cumulative	m(g)	m(g) ascending order	times	recount	mean(g)-m(g)	standard deviation
0,66	0,66	0,65	0	1	-0,045915493	0,002108232
1,44	0,78	0,66	1		0,074084507	0,005488514
2,21	0,77	0,66	1		0,064084507	0,004106824
2,89	0,68	0,66	1		-0,025915493	0,000671613
3,57	0,68	0,66	1		-0,025915493	0,000671613
4,29	0,72	0,66	1		0,014084507	0,000198373
4,95	0,66	0,66	1		-0,045915493	0,002108232
5,67	0,72	0,66	1	7	0,014084507	0,000198373
6,41	0,74	0,67	2		0,034084507	0,001161754
7,12	0,71	0,67	2		0,004084507	1,66832E-05
7,94	0,82	0,67	2		0,114084507	0,013015275
8,61	0,67	0,67	2		-0,035915493	0,001289923
9,28	0,67	0,67	2	5	-0,035915493	0,001289923
10,01	0,73	0,68	3		0,024084507	0,000580063
10,85	0,84	0,68	3		0,134084507	0,017978655
11,58	0,73	0,68	3		0,024084507	0,000580063
12,27	0,69	0,68	3		-0,015915493	0,000253303
12,96	0,69	0,68	3		-0,015915493	0,000253303
13,72	0,76	0,68	3		0,054084507	0,002925134
14,43	0,71	0,68	3	7	0,004084507	1,66832E-05
15,13	0,7	0,69	4		-0,005915493	3,49931E-05
15,85	0,72	0,69	4		0,014084507	0,000198373
16,52	0,67	0,69	4		-0,035915493	0,001289923
17,21	0,69	0,69	4		-0,015915493	0,000253303
17,99	0,78	0,69	4		0,074084507	0,005488514
18,74	0,75	0,69	4		0,044084507	0,001943444
19,49	0,75	0,69	4		0,044084507	0,001943444
20,2	0,71	0,69	4		0,004084507	1,66832E-05
20,89	0,69	0,69	4		-0,015915493	0,000253303
21,74	0,85	0,69	4		0,144084507	0,020760345
22,43	0,69	0,69	4	11	-0,015915493	0,000253303
23,15	0,72	0,7	5		0,014084507	0,000198373
23,83	0,68	0,7	5		-0,025915493	0,000671613
24,56	0,73	0,7	5		0,024084507	0,000580063
25,22	0,66	0,7	5		-0,045915493	0,002108232
25,91	0,69	0,7	5		-0,015915493	0,000253303

26,61	0,7	0,7	5		-0,005915493	3,49931E-05
27,31	0,7	0,7	5		-0,005915493	3,49931E-05
28	0,69	0,7	5	8	-0,015915493	0,000253303
28,69	0,69	0,71	6		-0,015915493	0,000253303
29,56	0,87	0,71	6		0,164084507	0,026923725
30,43	0,87	0,71	6		0,164084507	0,026923725
31,17	0,74	0,71	6	4	0,034084507	0,001161754
31,87	0,7	0,72	7		-0,005915493	3,49931E-05
32,59	0,72	0,72	7		0,014084507	0,000198373
33,31	0,72	0,72	7		0,014084507	0,000198373
34,01	0,7	0,72	7		-0,005915493	3,49931E-05
34,72	0,71	0,72	7		0,004084507	1,66832E-05
35,4	0,68	0,72	7		-0,025915493	0,000671613
36,08	0,68	0,72	7	7	-0,025915493	0,000671613
36,74	0,66	0,73	8		-0,045915493	0,002108232
37,43	0,69	0,73	8		-0,015915493	0,000253303
38,11	0,68	0,73	8		-0,025915493	0,000671613
38,79	0,68	0,73	8	4	-0,025915493	0,000671613
39,46	0,67	0,74	9		-0,035915493	0,001289923
40,18	0,72	0,74	9	2	0,014084507	0,000198373
40,87	0,69	0,75	10		-0,015915493	0,000253303
41,6	0,73	0,75	10	2	0,024084507	0,000580063
42,3	0,7	0,76	11	1	-0,005915493	3,49931E-05
43	0,7	0,77	12	1	-0,005915493	3,49931E-05
43,69	0,69	0,78	13		-0,015915493	0,000253303
44,52	0,83	0,78	13	2	0,124084507	0,015396965
45,32	0,8	0,8	15		0,094084507	0,008851894
46,12	0,8	0,8	15	2	0,094084507	0,008851894
46,78	0,66	0,82	17	1	-0,045915493	0,002108232
47,48	0,7	0,83	18	1	-0,005915493	3,49931E-05
48,14	0,66	0,84	19	1	-0,045915493	0,002108232
48,79	0,65	0,85	20	1	-0,055915493	0,003126542
49,46	0,67	0,87	22		-0,035915493	0,001289923
50,12	0,66	0,87	22	2	-0,045915493	0,002108232

ANNEX 2

ROUTINE "FIRST":

```
function [Fbvp4c,curvaturebvp4c,rcoal]=first(R,theta,V,h,gamma)
%res=[F,curvature,rcoalescence]

% 1 - DEFINITION OF USER PARAMETERS

% SYMMETRIC CASE!!! All parameters in SI units (MKS)
% Physical parameters
if nargin==0
    close all
    clear all
    clc
    R=1e-3;          % sphere radius
    theta=0/180*pi; % contact angle in rad
    V=1e-10;         % volume of liquid
    h=0e-6;             % distance between both spheres
    gamma=72e-3;     % surface tension
end

% Numerical parameters
n=100;%number of points of the meniscus
minvalue=eps;%minimal value of phi in the dichotomic search, phi is the
filling angle
maxvalue=30/180*pi;%maximal value of phi in the dichotomic search, phi is
the filling angle
tolvol=0.005;%relative tolerance on the volume of liquid to stop the
iterative simulation
tolphi=0.005;%relative tolerance on the filling angle to stop the
simulation, in case phi-->phimax or phi-->phimin (see later on)

% Cosmetic paramters
clcolor=[1 1 1]*0.3;
cllinestyle='none';%construction lines linestyle, 'none' for none, '--' for
dashed line

% 2 - BEGINNING OF THE SIMULATION

% Preparation to enter the loop
phimin=minvalue;
phimax=maxvalue;
interval=(maxvalue-minvalue);
phi=(phimin+phimax)/2;% first step of the dichotomic search, phi is
initialized in the middle of the [phimin,phimax] interval
go=1; %go=1 to (re)enter the loop, go=0 to stop at the end of the loop
count=0;%iteration counter

% Let's enter the loop
```

```
while go

    % A - Search an initial guess of the meniscus profile: the parabolic
    % model is a good candidate
    % r(z)=a0+a2*z^2 (z is the axis passing through both spheres centers)
    a2=geta2(phi,R,theta,h);
    a0=geta0froma2(phi,R,h,a2);

    % B - Preparation of the Boundary Value Problem resolution (bvp4c)
    % z varies - descending - between a=h/2+R*(1-cos(phi)) and b=0
    b=0;
    a=h/2+R*(1-cos(phi));
    zinit=linspace(a,b,n);
    % The boundary conditions are r(z=a)=rtop=R*sin(phi) and
    % r(z=0)=rbot(tom)=a0
    rbot=a0;
    rtop=R*sin(phi);
    rinit=[rbot rtop];
    % An initial guess for the curvature is given by the parabolic model

    Hinit=(1/a0-2*a2);

    % We now define the initial solution for the bvp4c problem
    binit=bvpinit(zinit,rinit,Hinit);

    % B - Definition of the boundary conditions
    bcfun = @(Ya, Yb, H)bndcond(Ya, Yb, H, rtop, theta, phi);

    % C - RUN of the resolution, i.e. the search of a meniscus
    % corresponding to the phi filling angle (we are in a loop...)
    % sol is a structure defined in the help of bvp4c
    sol = bvp4c(@(z, r, H)ODEcurvatureRofZ(z, r, H), bcfun, binit);
    % a bit of cosmetics...
    r=sol.y(1,:);
    z=sol.x;
    cl=plot(r,z,r,-z,-r,z,-r,-z);%cl=construction lines
    hold on
    set(cl,'linestyle',cllinestyle,'color',clcolor);

    % D - Estimation of the volume of liquid for the chosen phi
    [vbrut,vcap]=getVolume(r,z,R,phi);% vbrut=volume inside the meniscus,
vcap=volume inside the spherical cap defined by phi
    v=vbrut-vcap;

    % E - Dochotomic search condition
    % a bit of cosmetics
    count=count+1;
    if nargin==0
        disp(strcat('iteration=',num2str(count),',         v=',num2str(v),',
vbrut=',num2str(vbrut),' vcap=',num2str(vcap),', phi=',num2str(phi)));
    end
    % stopping condition: the volume of liquid is within the interval
```

```
    % defined by tolvol
    if (v>V*(1-tolvol))&&(v<V*(1+tolvol))
        go=0;
        disp('...');
        disp(strcat('Simulation stops because :',num2str(V*(1-
tolvol)),'<v=',num2str(v),'<',num2str(V*(1+tolvol))));
    elseif (v<V)%increase phi
        phimin=phi;
        phi=(phimin+phimax)/2;
    else %v>V, decrease phi
        phimax=phi;
        phi=(phimin+phimax)/2;
    end

    % stopping condition: phi has reached the extremities of its interval
[minvalue,maxvalue] without finding a solution
    if phi>maxvalue*(1-tolphi)
        go=0;
        disp(strcat('Simulation stops because phi=',num2str(phi)',' larger
than maxvalue*(1-tolphi)'));
    elseif phi<minvalue+interval/2*tolphi
        go=0;
        disp(strcat('Simulation stops because phi=',num2str(phi)',' smaller
than minvalue+interval/2*tolphi'));
    end
% go=1: we reloop
% go=0: we stop
end

% The solution is - if reached - contained in the struct sol

% 3 - POST-TREATMENT
% Display

meniscus=plot(r,z,r,-z,-r,z,-r,-z);
set(meniscus,'linewidth',2,'color','b');
draw(a0,a2,R,h,phi);%spheres and parabolic meniscus

% Forces computation
apex_radius=r(end);
curvature=sol.parameters;%curvature=2H=dp/gamma
FT=-2*pi*apex_radius*gamma %tension force
FL=pi*apex_radius^2*curvature*gamma%laplace force
F=FT+FL;%capillary force
% if needed, the benchmark with Israelachivili: don't forget to set h=0 and
% V small enough to have phi so small that phi=sin(phi)
Req=(1/R+1/R)^(-1);
Fisra=-4*pi*Req*gamma*cos(theta);
% forces through the parabolic model...
FTparabol=getFT(a0,a2,gamma);
FLparabol=getFL(a0,a2,gamma);
Fparabol=FTparabol+FLparabol;
```

```
% Results display in the command window
if nargin==0
disp('...parameters (SI units)')
disp(strcat('R=',num2str(R)));
disp(strcat('h=',num2str(h)));
disp(strcat('V=',num2str(V)));
disp(strcat('theta=',num2str(theta/pi*180),'°'));
disp('...');
disp(strcat('Force by numerical integration (in N, negative is
attractive)=',num2str(F)));
disp(strcat('Force by Israelachvili approximation (in N, negative is
attractive)=',num2str(Fisra)));
disp(strcat('Force by parabolic model (in N, negative is
attractive)=',num2str(Fparabol)));
disp('...')
disp(strcat('Filling angle phi (in rad)
=',num2str(phi)));
else
    disp(strcat('Force by numerical integration (in N, negative is
attractive)=',num2str(F)));
end

% outputs
Fbvp4c=F;
curvaturebvp4c=curvature;
rcoal=r(1);

%--------------------------------------------------------------------------
%    Auxiliary functions
%--------------------------------------------------------------------------

function res = bndcond(Ya, Yb, curvature, rtop, theta, phi) %#ok
    res = [Ya(1) - rtop; Ya(2) - tan(pi/2 - phi- theta); Yb(2)];

function dr = ODEcurvatureRofZ(z, r, curvature)
dr = [r(2); (1 + r(2)^2)^1.5 * (-curvature + (1 + r(2)^2)^-0.5 / r(1))];

function [Vbrut,Vcap]=getVolume(r,z,R,phi)
Vcap=2*2*pi*R^3/3*(1-1.5*cos(phi)+0.5*(cos(phi))^3);
Vbrut=2*pi*trapz(-z,r.^2);

function res=myfun(phi,R,theta,h)
% compute the volume of liquid
a2=geta2(phi,R,theta,h);
a0=geta0froma2(phi,R,h,a2);
Vcap=2*pi*R^3/3*(1-1.5*cos(phi)+0.5*(cos(phi))^3);%volume of a spherical
cap
zA=h/2+R*(1-cos(phi));%A is the point where the meniscus reaches the upper
sphere
res=2*pi*(a0^2*zA+2*a0*a2/3*zA^3+a2^2*zA^5/5)-2*Vcap;%volume of liquid
```

```
function a0=geta0froma2(phi,R,h,a2)
% computes the apex radius of the meniscus
zA=h/2+R*(1-cos(phi));
a0=R*sin(phi)-a2*zA^2;

function a2=geta2(phi,R,theta,h)
% no physical meaning, excepted that a2 is related to the parabolic
% meniscus curvature
zA=h/2+R*(1-cos(phi));
a2=tan(pi/2-theta-phi)/(2*zA);

function FT=getFT(a0,a2,gamma)
% parabolic model
FT=-2*pi*a0*gamma;

function FL=getFL(a0,a2,gamma)
% parabolic model
p=gamma*(1/a0-2*a2);
FL=pi*a0^2*p;

function draw(a0,a2,R,h,phi)
theta=linspace(0,2*pi,1000);
rc=R*cos(theta);
zc=h/2+R+R*sin(theta);
circles=plot(rc,zc,'k',rc,-zc,'k');
set(circles,'linewidth',2);

zpar=linspace(-h/2-R*(1-cos(phi)),h/2+R*(1-cos(phi)),20);
rpar=a0+a2*zpar.^2;
parabola=plot(rpar,zpar,-rpar,zpar);
set(parabola,'color','r','linewidth',1.5);

axis equal
set(gcf,'color','w');
xlabel('r (m)');
ylabel('z (m)');

theta
```

ROUTINE "SECOND":

```
function second
close all

R=1e-3;
theta=50.598/180*pi;
h=0;
gamma=72e-3;
ua=101325;
```

```
%Xsi=[0.0001 0.001 0.005 0.01 0.02 0.05 0.1];
Xsi=linspace(0.0001,0.3,30)
%interstitial_volume=(2*R)^3*(sqrt(2)-pi/3);  %empilement  compact  (closed
pack-wikipedia)
interstitial_volume=2*pi*R^3-(4/3)*pi*R^3
volume=interstitial_volume*Xsi; % liquid volume

figure
for i=1:length(Xsi)
    V=volume(i)
    [Fbvp4c,curvaturebvp4c,rcoal]=first(R,theta,V,h,gamma)
    F(i)=Fbvp4c %capillary force between two spheres
    hold on
    uw(i)=curvaturebvp4c*gamma+ua  %water  pressure  (air  pressure  ua  =
101400Pa)
    correction(i)=Xsi(i)*(ua-uw(i)) %literature correction
end

figure
p=plot(Xsi,correction);
set(p,'color','r','marker','o');
set(gcf,'color','w');
xlabel('\Xi');
ylabel('Correction (Pa)');
```

ANNEX 3

CONTACTS

This appendix lists the different suppliers and contact's involved in the setup of the test bench.

1. Dehaye (General mechanical tools)
   Rue Georges Moreau, 57
   B-1070 Bruxelles
   Belgium
   www.dehaye.com

2. Eppendorf (Manual droplets dispensing device)
   Belgian dealer:
   Fisher Bioblock Scientific
   Patrick Cogez (Belgium@bioblock.com)
   BP 567
   B-7500 Tournal 1
   Belgium
   - Pipette Research 0.1-2.5µL, Ref. 3111000114

3. Keyence
   Patrick De Volder (info@SensingSolutions.be)
   - CCD camera CV500 (with CV050)
   - Displacement sensors LC-2440

4. Newport N.V.
   Arjan Bos (Netherlands@nexport-nl.com)
   Tiranastraat, 25
   3404 CJ Ijsselstein
   The Netherlands
   - Translation stages (X) M-SDS40
   - Translation stages (XY) M-DS40-XY
   - Rotational stage M-RS40
   - Breadboard 60cmx60cm M-EG-22-2

5. Precision Brand (Steel beams, finally not used)
   Belgian dealer: Ets Dehaye
   - Steel feeler gage 0.102mmx5'' (n°UPC19230)

6. SMAC (Linear actuator used to test dynamical release)
   Jos Mooren
   smacnl@tiscali.nl

Tel: 00 31 (0) 6 537 63 4 63
Technical Support Manager
Stepekolk Oost 3
5706 LA Helmond
www.smac-mca.com

- LAL95-15

7. Vision Light Tech B.V. (Back light system)
   Paul Van Der Velde (pvdv@vlt.nl)
   Protonenlaan, 22
   5405 NE Uden
   The Netherlands P.O. Box 345
   www.machine-vision.nl
   - Back light system LDLTP83x75
   - Power Supply PD-3012
   - Band pass filter BP660-30.5
   - Cables CB-2

8. Brabant (steel balls)
   Chaussée de Mons 1135
   1070 Bruxelles
   Tel. 02 529 01 01
   Fax 02 529 01 00
   brabant@brammer.biz

9. SENSY-Sensors and Synergy SA
   Force captor 200 Kg Model 2712
   Output 2, 0400 m V/V CAP 200 daN
   Serial n° 2000441015